Material Processing for Edible Electronics

by

Wenwen Xu

A Dissertation Presented in Partial Fulfillment
of the Requirements for the Degree
Doctor of Philosophy

Approved November 2018 by the
Graduate Supervisory Committee:

Hanqing Jiang , Chair
Lenore L. Dai
Matthew Green
Bin Mu
Hongbin Yu

ARIZONA STATE UNIVERSITY

May 2019

ABSTRACT

A new type of electronics was envisioned, namely edible electronics. Edible electronics are made by Food and Drug Administration (FDA) certified edible materials which can be eaten and digested by human body. Different from implantable electronics, test or treatment using edible electronics doesn't require operations and perioperative complications.

This dissertation bridges the food industry, material sciences, device fabrication, and biomedical engineering by demonstrating edible supercapacitors and electronic components and devices such as pH sensor.

Edible supercapacitors were fabricated using food materials from grocery store. 5 of them were connected in series to power a snake camera. Tests result showed that the current generated by supercapacitor have the ability to kill bacteria. Next more food, processed food and non-toxic level electronic materials were investigated. A "preferred food kit" was created for component fabrication based on the investigation. Some edible electronic components, such as wires, resistor, inductor, etc., were developed and characterized utilizing the preferred food kit. These components make it possible to fabricate edible electronic/device in the future work. Some edible electronic components were integrated into an edible electronic system/device. Then edible pH sensor was introduced and fabricated. This edible pH sensor can be swallowed and test pH of gastric fluid. PH can be read in a phone within seconds after the pH sensor was swallowed. As a side project, an edible double network gel electrolyte was synthesized for the edible supercapacitor.

Dedication

I dedicate my dissertation work to my family. I present a special feeling of gratitude to my loving parents, Baoxiang Xu and Eryun Wang whose words of encouragement and push for tenacity ring in my ears. I also dedicate this dissertation to my husband, Zeming song, for the unconditional love and support he has for me. I also specially dedicate this dissertation to my son Evan. You have made me stronger, better and more fulfilled than I could ever imagined.

ACKNOWLEDGMENTS

I would like to first express my deepest gratitude to my supervisor, Prof. Hanqing Jiang, who has always been supportive, helpful and caring ever since I entered his group at Arizona State University. His vision, leadership and perseverance for research have been the constant driving force for my progress. I feel very fortunate to have been his student, and therefore to have had such an enjoyable and fulfilling graduate school experience.

I would also like to deeply thank Prof. Lenore L. Dai, who were abundantly helpful and offered invaluable assistance and guidance to the synthesis of yolk-shell structure projects. I am also grateful for her insightful comments and crucial remarks that shaped my final dissertation.

I also love to thank Prof. Hongbin Yu who have been advising me on edible electronics project and sharing with me his tremendous experience in the electric circuit field.

In addition, I am very grateful for all the help and advice from my committee members, Prof. Matthew Green and Prof. Bin Mu.

Last but not the least, the help and support from my colleagues at Arizona State University, Dr. Prithwish Chatterjee, Dr. Xu Wang, Haokai Yang, Dr. Elizabeth M Nofen, Yifei Xu, Dr. Cheng Lv, Dr. Wei Zeng, Yi Yang, Todd Houghton, Korinthia Yuriar-Arredondo, Dr. Mitchell R Armstrong, Bohan Shan, Vaasavi Sundar and Rishi Choksiare are truly appreciated.

TABLE OF CONTENTS

Page

CHAPTER Page

LIST OF TABLES

LIST OF FIGURES

Figure Page

Figure Page

Figure Page

Figure Page

Figure Page

Figure Page

Figure Page

CHAPTER 1 GENERAL INTRODUCTION OF MEDICAL ELECTRONICS

Novel and innovative medical technologies and devices have emerged to treat various diseases, such as deep brain stimulators for Parkinson's diseases (*1*), vagal nerve stimulators for epilepsy (*2*), electronic aspirin for head or facial pains (*3*), and insulin pumps for diabetes (*4, 5*).

Implantable medical electronics can monitor and treat physiological conditions within human body. They are critically requested for the survivals of patients who suffer from certain diseases such as bradycardia, fibrillation, disease of digestive tract and disability, etc. The electronics include cardiac pacemaker (*6*), cardiac defibrillators, drug delivery system and neurostimulators and so on. At least 2 surgeries are needed to implant the device into body and replace a new one. Surgeries cannot be avoided since the electronics need to be implanted into human body.

Besides the traditional implantable medical electronics, the ‘camera in a pill’ is a development that is generating considerable interest. This new kind of implantable medical electronics doesn’t need any surgery. There is a less than 1% chance that the patient will require surgical intervention to retrieve the capsule (*7*). Wireless capsule endoscopy was first reported 16 years ago when a paper in Nature described the development of a disposable capsule that takes pictures during its course through the digestive tract after being swallowed (*8*). The highly impacted wireless endoscopy system consists of three components: the capsule camera, external receiving antenna and portable hard drive worn by the patient during the examination. No medicine or surgery is needed for this examination, unlike the conventional endoscopy (*7*). Beside taking images in

gastrointestinal (GI) tract (*7*, *9*), capsules are also under way to be developed with different functions, such as measure pH (*10*), temperature (*11*) and pressure (*12*).

Although implantable electronic devices have revolutionized the care of patients, they harbor shortcomings such as the need for operations and perioperative complications. Biodegradable electronics and recent bioresolvable devices, such as individual transistors (*13*), primary battery and biosensors (*14-18*), and organic field effect transistors (*19-21*), provide an alternative option to implantable electronics. Biodegradable medical electronics significantly expand the functional capabilities in medicine. Only one surgery is needed to implant the biodegradable medical electronic into human body and the electronic will be degraded by blood, body fluid and tissue fluid etc.

Biodegradable electronics mainly built using biocompatible and biodegradable materials provide multifunctional operation to assist or monitor a biological event or release drug and cure disease. Biodegradable power supply is an essential part for the electric systems. Primary batteries have multiple types to meet different specific demand such as pulsed high energy, continuous low current and so on. Yin et al. (*18*) reported a biodegradable primary battery with all degradable, environmentally friendly and biocompatible materials as component. Magnesium foils work as the anodes, while metal foils based on iron (Fe), tungsten (W) or molybdenum (Mo) serve as the cathodes, and the packages are polyanhydrides. Another example of biodegradable electronics is organic field effect transistors (OFETs). Biocompatible, biodegradable and ingestible electronics circuits and capsules for medical diagnosis, monitoring, drug delivery and healing are currently based on traditional silicon technology. Such medical electronics were ideally fabricated with natural material or biodegradable-biocompatible polymers.

Transistors with an operational voltage of 4-5 V, a source drain current of up to 0.5 A and an on-off ratio of 3-5 orders of magnitude have been fabricated with such materials (*19*). First trial to make a partially biodegradable field effect transistor was fabricated with polyvinyl alcohols (as gate dielectric), 5-5'-bis-(7-dodecyl-9H-fluoren-2yl)-2,2'-bithiophene (DDFTTF) (as organic semiconductor) and poly(L-lactide-co-glycolide) (PLGA) (as substrate). Later, more materials were discovered to have the potential to make biodegradable transistors. Ecoflex made from potato and corn starch and edible hard gelatin capsule produced from collagen or caramelized glucose was served as the biodegradable substrate. Aurin as rosolic acid which is derived from Plantago Asiatica L. acts as the smoothing layer. Aurin has been widely investigated in the medical and pharmacological field (*29*). Other natural materials such as lactose, glucose, sucrose and guanine have been used as dielectric in biochemistry for a long time (*19*). Transistors and integrated circuits from natural or nature-inspired materials may ultimately provide the basis for "green electronics."

Although biodegradable electronics resolve the issue of repeat surgery, they have other inherent shortcomings, such as limitations with structural materials and properties. In addition to implantation of permanent and biodegradable devices, the digestive system may serve as another route for administration of electronics that can modulate cellular and organ function without the need for implantation. Although some groups have proposed edible materials in the past, these materials still contain toxic components (*30-33*). Human dependence on food and digestion for over 200,000 years of evolution has allowed us to optimize timing and passage of materials through the alimentary tract. The

merit of employing materials from food to develop edible electronics is apparent: they are explicitly edible.

The next chapter uses the accumulated knowledge in the food industry, material sciences, device fabrication, and biomedical engineering and demonstrates fully functional and edible supercapacitors with the potential to work in the alimentary tract. Instead of using traditional noninert metals (e.g., iron, magnesium, and zinc), dielectric, and semiconducting materials (e.g., silicon) that can only be taken in very tiny amount at the level of micrograms per day, electrically conductive and chemically stable carbon (in the form of activated charcoal) and inert metals (edible gold), as well as other food sources were adopted in the fabrication of edible supercapacitors. The next chapter studied some edible materials and their performance as components for a supercapacitor. Most importantly, for the first time, a single edible supercapacitor in the size of a standard capsule was demonstrated to possess enough energy and power to function as a standalone device to exhibit antibacterial activity by killing disease-causing bacteria in vitro. Also, as energy storage device, these supercapacitors are demonstrated to connect in series are sufficiently powerful to drive a commercial camera.

In the third chapter, a preferred food kit was established for fabricating edible components and device. Furthermore, this dissertation will introduce the fabrication process of more edible components such as conductor, resistor, capacitor and devices such as pH sensor and discuss results in detail in the rest chapters.

CHAPTER 2 EDIBLE SUPERCAPACITORS

2.1. Background and Motivations

Supercapacitor, an energy storage device through electrochemical methods, which is also known as ultracapacitor or electrochemical capacitors, are considered as the most promising candidate for energy storage due to its high power energy, long cyclic life (>100,000 cycles), rapid charge-discharge rate, and environmental friendly (*34*). Farad is a unit of capacitance named after the English physicist Michael Faraday (1791–1867). One farad stores one coulomb of electrical charge when applying one volt. One microfarad is one million times smaller than a farad, and one pico-farad is again one million times smaller than the microfarad. Engineers at General Electric first experimented with an early version of supercapacitor in 1957, but there were no known commercial applications. In 1966, Standard Oil rediscovered the effect of the double-layer capacitor by accident while working on experimental fuel cell designs. The double-layer greatly improved the ability to store energy. The company did not commercialize the invention and licensed it to NEC, who in 1978 marketed the technology as "supercapacitor" for computer memory backup. It was not until the 1990s that advances in materials and manufacturing methods led to improved performance and lower cost. All capacitors have voltage limits. While the electrostatic capacitor can be made to withstand high volts, the supercapacitor is confined to 2.5–2.7V. Voltages of 2.8V and higher are possible, but at a reduce service life. To get higher voltages, several supercapacitors are connected in series. Serial connection reduces the total capacitance and increases the internal resistance.

Most of medical devices are using supercapacitor as the energy source. However, since they consist of toxic materials, a surgery is still needed to replacing the exhausted electronics with a new one or taking the supercapacitor out from human body. To provide continuous supplied energy for implantable or edible devices, a non-toxic edible and digestible supercapacitor is highly desired.

The supercapacitor has evolved and crosses into battery technology by using special electrodes, packaging material, separator and electrolyte. Most of those materials are toxic and cannot be eaten. Herein edible supercapacitors exhibited in vitro antibacterial activity and power a snake camera was demonstrated. All materials involved are explicitly originated from edible food products, such as activated charcoal, seaweed, polyelectrolyte drink, rice paper, egg, gold leaf, cheese and so on. This study represents a new era of edible electronics with the potential to revolutionize modern biomedical technologies and devices.

2.2. Experimental Section

2.2.1. Fabrication of edible supercapacitors

The slurry was prepared by mixing the activated charcoal (Nature's Way Products, Inc; Green Bay, WI) with egg white in a mass ratio of 1:2. Egg whites primarily contain biotin and proteins such as albumin, mucoproteins, and globulins that are able to form a biomacromolecule solution with water through hydrogen bonding between the proteins and water. Deionized water was then added into the mixture with a ratio of 1:3 (activated charcoal to water). The mixture was magnetic stirred for 2 hr followed by an ultrasonication for 30 minutes in water bath. The current collector was prepared by

applying egg white uniformly on chlorine-free wood fiber paper (Mondi; Graz-Seiersberg, Austria) to form an adhesive layer, then attaching ~3 μm thick 23 kt edible gold leaf (Alma Gourment Ltd; Long Island City, NY) on the paper. The gold-coated paper was then dried in ambient environment for 2 h before being patterned into the current collector with desired areas. The slurry was coated on the current collector by doctor's blading followed by overnight drying in ambient environment and 6 h drying in room temperature, low pressure (10 Pa) chamber to avoid thermal stress as well as remove the water in the electrode. Figure 2.2 shows the image of a patterned and coated electrode (2 cm × 2 cm). A typical thickness of the electrode is 120 μm. Roasted seaweed (Nagai NoRi Co., Ltd; Torrance, CA), a popular snack and also heavily used in sushi, was used as one of the possible separators. Seaweed consists of multilayer hydrophilic structures with high electrical resistivity and high ion permeability. Finally, the supercapacitor was assembled by laminating roasted seaweed (Nagai NoRi Co., Ltd; Torrance, CA) as separator between two electrodes and thermal sealing of gelatin sheets as package (Modernist Pantry, LLC; York, ME). Between the gelatin sheets and collectors, cheese slices were placed to avoid the absorption of electrolyte by gelatin. Fig 2.2 (b) shows the collection of foods that were used in making the edible supercapacitors.

2.2.2. Electrochemical measurements

Charge-discharge tests were performed using Arbin electrochemical workstation. The galvanostatic voltage range was –0.8-0.8 V. The specific capacitance (C_{sp}) was calculated from the slope of the discharge capacitance $C_{sp} = \frac{2I}{m(\frac{\Delta V}{\Delta t})}$, where I is the applied current and m is the average mass of the two electrodes. Electrochemical impedance

spectroscopy (EIS) studies were performed by applying a small perturbation voltage of 5 mV in the frequency range of 0.01 Hz to 100 kHz. The energy and power density were calculated by conducting galvanostatic charge–discharge cycling with constant current densities ranging from 250 mA/g to 4 A/g. Cyclic voltammentry (CV) was tested in potentiostats (Gamry Potentiostats Reference 300) from –0.8-0.8 V.

2.2.3. Field scanning electron microscopy (FESEM)

The activated charcoal electrode and seaweed were initially dried at 150 ℃ to remove any moisture from the surface. Then they were deposited gold for 10min in Au target sputter. The cross-section of activated charcoal electrode and the morphology of seaweed were observed using scanning electron microscopy (Hitachi S4700 FESEM).

2.2.4. Brunauer–Emmett–Teller (BET) test

The activated charcoal used as the supercapacitor electrodes was initially dried at 150 ℃ to remove any moisture from the surface. The adsorption analysis was carried out with a Micromeritics ASAP2000. Specifically, 0.1 grams of the activated charcoal was loaded in the tube with nitrogen flowing at 2 bar pressure for 4 h. Adsorption was analyzed using the BET module. The results revealed a surface area of ~1,400 m^2/g for the activated charcoal (Figure 2.1 (d)).

2.2.5. Permittivity test

The seaweed and rice paper were studied for their permittivity using deionized water as the passing fluid. Briefly, 2-inch diameter sections of seaweed and rice paper were cut

out using a circular stamp. The testing material (i.e., seaweed and rice paper) was placed at the end of a 5-inch steel chamber using a rubber gasket. Water was poured into the chamber, and the sequential pressure test was performed using regulated nitrogen from a cylinder. The fluid passing out from the chamber was collected in a beaker and placed on a weighing balance, which was connected to a computer. The data from the fluid pass was used to calculate mass flux and permittivity.

2.2.6. In-situ 2D observation of gelatin sheet digestion in simulated gastric fluid

A gelatin sheet with dimensions of 160 μm (thickness) × 1,090 μm × 4,000 μm was used for the observation. Figure 2.3 presents the experiment setup. The gelatin sheet was held vertically by a sponge stage in a glass dish under an optical microscope. The sponge stage was able to keep the gelatin sheet standing in the glass dish and impose mechanical constraints in the horizontal direction. The simulated gastric fluid was composed of 2.0 g of sodium chloride and 3.2 g of purified pepsin (derived from porcine stomach mucosa, with an activity of 800 to 2,500 units per mg of protein) in 7.0 mL of hydrochloric acid (HCl) and water (1000 mL). This test solution has a pH of about 1.2. When the sponge was soaked with simulated gastric fluid and touched the gelatin sheet, it could be used to simulate the gelatin sheet in stomach environment. After the simulated gastric fluid was poured into the glass dish, swelling and digestion of the gelatin sheet were observed *in-situ* by microscopy (Nikon eclipse lv100). It was observed that a gelatin sheet with an initial cross-sectional area of 160 μm × 1,090 μm first swells due to the diffusion of the gastric fluid into the polymeric gelatin network, and then shrinks due to the digestion of gelatin and eventually becomes undetectable microscopically (Nikon eclipse lv100, 5X

objective) after 2.5 h. During this process (swelling → shrinking), because of the constraint in the horizontal direction, the maximum strain in the horizontal direction $\varepsilon_{horizontal}$ was only 17%, while its counterpart in the thickness direction $\varepsilon_{thickness}$ was 261%. This quasi-one-dimensional constrained digestion process can be understood by a theoretical model that considers the coupling of mass diffusion, chemical reaction, and extremely large mechanical deformation.

2.2.7. Other food materials for edible supercapacitor

Table 2.1 shows materials (food) that have been studied as components of the edible supercapacitors. For columns,

(1) Binders: In addition to egg white, CMC, a cellulose derivative with carboxymethyl groups bound to the hydroxyl groups of the glucopyranose monomers that make up the cellulose backbone, has also been applied as binder. CMC is widely used in the food industry as a viscosity modifier, thickener, or stabilizer to stabilize emulsions and serve as a binder.

(2) Current collectors: In addition to gold leaves, silver leaves were also used. Both gold and silver leaves are used for decorating cakes.

(3) Electrolytes: Besides Gatorade sports drink, lemon juice, Monster energy drink, and V8 vegetable juice have been studied as possible electrolytes. All of these drinks contain large amounts of transportable free sodium or potassium ions and anions. Moreover, a surprising discovery is that the homemade jello, cheese, and BBQ sauce work efficiently as electrolytes. For jello and cheese, separators are not needed, since these food products are efficient electrolytes. In order to increase the ionic concentration,

monosodium glutamate (MSG) has been added as an electrolyte additive. MSG is the sodium salt of glutamic acid, commonly used in the food industry as a flavor enhancer.

(4) Separators: In addition to seaweed, rice paper was also studied as a separator. Both seaweed and rice paper have the ability to maintain electrolytes and allow the transportation of ions.

(5) Segregation layer: For all liquid electrolytes, cheese was selected as segregation layers. For solid electrolytes, the segregation layer is not needed.

(6) Packaging materials: Gelatin and gummy candy were served as packaging materials.

2.2.8. Edible supercapacitor lighting up light-emitting diodes (LED)

The supercapacitor set consists of three supercapacitors connected in series. The electrode area is 2 cm × 2 cm with an average mass loading of 0.02 g. For LED lighting inside simulated gastric fluid, two-thirds of the supercapacitor body was immersed in the fluid. The LED stayed on for three minutes, followed by gradual dimming and lack of emission after four minutes. After one h, the supercapacitor was partially dissolved in the simulated gastric fluid. For LED lighting outside simulated gastric fluid, two-thirds of the supercapacitor body was immersed in the fluid. The LED stayed on for 10 minutes.

2.2.9. Wireless charging system

The wireless charging system consists of a transmitter chamber, in which supercapacitors will be placed, and a receiver lid, with which supercapacitors will be connected. The transmitter chamber was fabricated by winding 17 turns of copper wire

on the outside wall of a glass tube (diameter 72.2 cm, height 40.1 cm). A transmitter circuit (GHH, Amazon) was then connected with coil and taped on the wall. The main function of the transmitter circuit is to convert direct current to alternating current with a frequency of 60 Hz. Thus, an alternating electromagnetic field will be created in this chamber by the alternating current. The receiver lid was fabricated by winding 19 turns of copper wire on the surface of a lid made of rice paper and copy paper. 2 more turns was used in the receiver end to increase the reliability of the system and to ensure that the 5V signal to transmitter end will be fully received. A receiver from the same transmitter-receiver module (GHH, Amazon) was then mounted at the center of the lid and connected with the receiver coil. The supercapacitor can be connected with the receiver lid through the two openings on the lid.

2.2.10. Edible supercapacitor charged in wireless charging system

Five supercapacitors (electrode area 4 cm $\times$ 4 cm) connected in series were placed in the charging chamber and initially connected with the receiver lid of the wireless charging system (Figure 2.8 (a)). Before charging, the supercapacitors were discharged to less than 0.5 V (Figure 2.8 (b)). The supercapacitor set was not able to light up the LED after the initial discharge. The supercapacitor set was then charged by connecting a 5V constant voltage source to the transmitter of the wireless charging system on the outside wall of the charging chamber. It was also connected with a voltage meter to monitor and record voltage changes during charging. After 5 minutes of constant voltage charge, the supercapacitor set reached 5V (Figure 2.8 (c)) and was able to light up the LED (Figure 2.8 (d)). The supercapacitor was then disconnected from the receiver of the wireless

charging system and removed from the charging chamber (Figure 2.8 (e)). The removed edible supercapacitor set was shown to light up the LED (Figure 2.8(f)).

2.2.11. Antimicrobial susceptibility testing with edible supercapacitor

The electrode dimension used in the supercapacitor-bacterial susceptibility experiments was 2 cm × 4 cm. The seaweed separator was first soaked with Gatorade electrolyte and then laminated between two electrodes. Subsequently, the entire sandwiched structure was curled into a roll and inserted into a standard 000 size gelatin capsule body (diameter 9.55 mm). The two current collector tabs were pulled out through the two openings on the capsule cap. Finally, both openings were sealed by edible birthday candle wax (LolliZ Co.; Poway, CA).

Exponential phase cultures of *Escherichia coli* ATCC 25922 were prepared by diluting overnight cultures into cation-adjusted Mueller Hinton broth, followed by growth to an OD_{600} of ~0.09 (~10^7 CFU/ml) at 37 ℃ with gentle rotary mixing. The cells were twice pelleted by centrifugation and resuspended in a phosphate-buffered saline solution (PBS). The cells were transferred to a 40 ml cylindrical glass tube, and current was introduced to the medium via the supercapacitor. A growth control, without supercapacitor-driven electrical current, was used to establish bacterial viability in PBS.

Two brass rods, held secure with a rubber stopper, were inserted into the 3 mL *E. coli* suspension in a vial. The electric current loop was formed by connecting the outside ends of the rods with the supercapacitor. A current release cycle consisted of a current pulse stage by connecting with supercapacitor for two minutes followed with a rest stage by disconnecting the supercapacitor for another two minutes. All experiments were

performed in a 37 ℃ warm room. Bacterial samples were collected every 15 min for 60 min. Bacterial cell survival was determined by plating duplicate 10-fold serial dilutions for each sample on Mueller Hinton agar and enumerating colonies on plates following overnight incubation at 37 ℃.

2.3. Results and discussion

Figure 2.1 (a) shows a schematic illustration of a representative supercapacitor in the explosive view, which contains package, current collectors, electrode materials, electrolyte, and separator. All components originate from food, which is also detailed in Figure 2.1 (a) as an example. The patterned electrode and collection of all materials (i.e., all food) are provided in the Figure 2.2. A photograph of an opened supercapacitor is shown in Figure 2.1 (b), with the activated charcoal as the electrode, seaweed as the separator, and cheese as the segregation layer. Taking the food shown in Figures 2.1 (a) and 3.1 (b) as an example, here activated charcoal (Nature's Way Products, Inc; Green Bay, WI) from dietary supplement capsules was used as electrode materials. Figure 2.1 (c) shows the transmission electron microscopy (TEM) image of activated charcoal, revealing that the size of an individual carbon particle is around 100 nm. As seen in Figure 2.1 (d), the surface area of the activated charcoal is approximately 1,400 m^2/g, which is comparable to activated carbon materials used in the majority of supercapacitors (*35*). In order to bind discrete active charcoal particles into a continuum film as electrodes, edible binders are employed. Egg white, widely used binding additives in food processing, were used as binders in electrodes. The presence of hydrogen bonds and ionic interactions with proteins allows the formation of films with high adhesive strength

(*36-38*), which allows egg whites to be used as binders in food processing industries. The edible metals, such as very thin gold and silver leaves that appear in artisan baking and many Eastern cuisines, are used as current collectors. The sheet resistance of the gold leaf with a thickness of 3-5 μm was measured to be 0.48 Ω/sq by four-point probe. Figure 2.1 (e) shows the scanning electron microscope (SEM) image of the electrode cross-section with a typical thickness of 120 μm. The separator needs to be permeable to ions and display high electrical resistance to avoid the electrical contact between the electrodes. Here, roasted seaweed, a popular snack and also heavily used in sushi, with multilayer hydrophilic structures served as one of the possible separators. Figure 2.1 (f) shows the SEM image of the roasted seaweed in a cross-sectional view, where the multilayer structures is seen. The permittivity of the roasted seaweed was measured to be 52 g/m^2s.

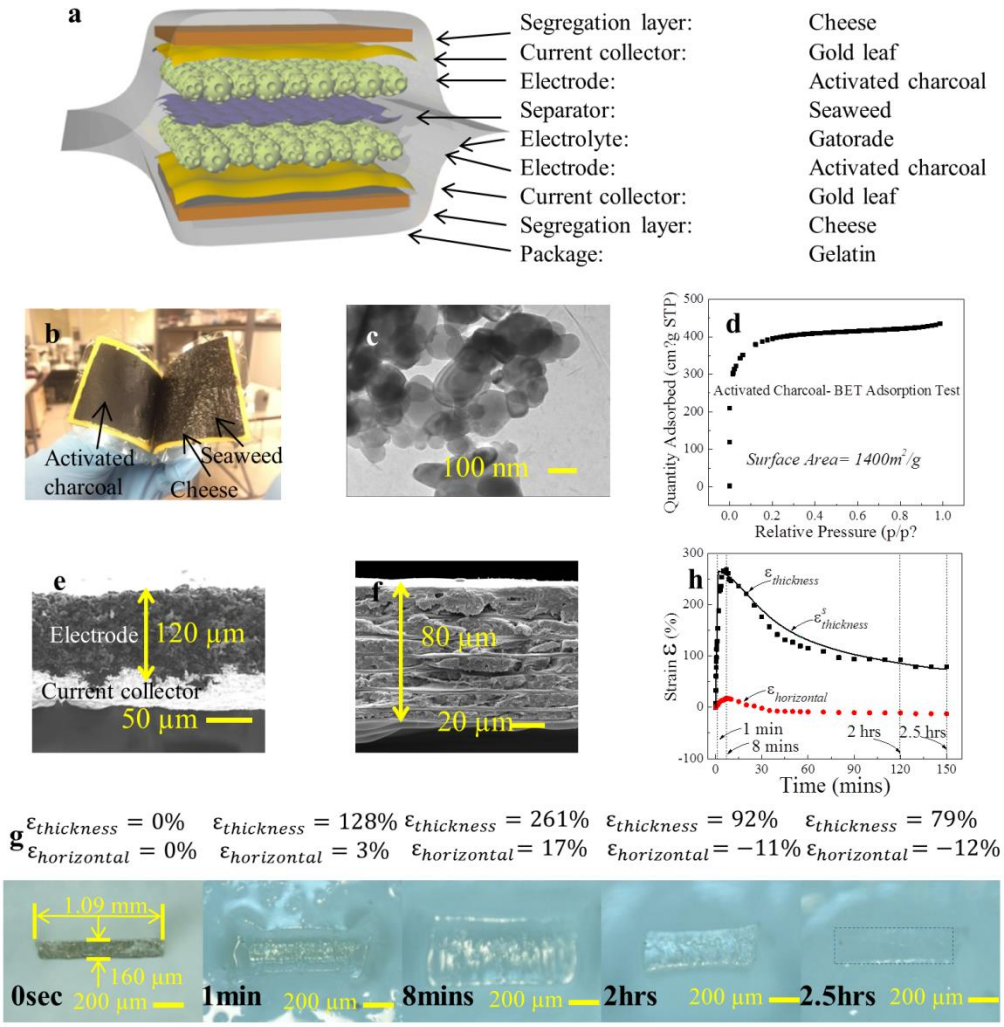

Figure 2.1 Illustration and materials analysis of the edible supercapacitor. (a) Schematic structural illustration of an edible supercapacitor. (b) An opened supercapacitor showing the activated charcoal electrode, seaweed separator, and gelatin package. (c) TEM image showing that the particle size of activated charcoal is about 100 nm. (d) Brunauer-Emmett-Teller (BET) test demonstrating the surface area of the activated charcoal is approximately 1,400 m^2/g. (e) SEM image of the cross-section of activated charcoal electrode. (f) Cross-section photograph of seaweed separator showing the multilayer-structure. (g) Dissolution test of the gelatin in simulated gastric fluid. (h) The time evolutions of the strains obtained from experiments and simulations.

Figure 2.2 (a) Image of a patterned electrode. (b) Material sources for edible supercapacitor, including cheese slices, activated charcoal capsules, Gatorade, egg white, gold leaves, seaweed, and gelatin sheets.

Gelatin sheets (Modernist Pantry, LLC; York, ME), used in food processes and many medical capsules, were employed as the package materials. Figure 2.1 (g) shows a cross-sectional view of an *in-situ* observation of a digestion process when a gelatin sheet was immersed in the simulated gastric fluid and constrained in the horizontal direction (Figure 2.3). It is observed that a gelatin sheet with an initial cross-sectional area of 160 μm × 1,090 μm first swells due to the diffusion of the gastric fluid into the polymeric gelatin network, and then shrinks due to the digestion of gelatin and eventually becomes undetectable microscopically (Nikon eclipse lv100, 5X objective) after 2.5 h. During this process (swelling → shrinking), because of the constraint in the horizontal direction, the maximum strain in the horizontal direction $\varepsilon_{horizontal}$ is only 17%, while its counterpart in the thickness direction $\varepsilon_{thickness}$ is 261%. This quasi-one-dimensional constrained digestion process can be understood by a theoretical model that considers the coupling of mass diffusion, chemical reaction, and extremely large mechanical deformation. As

shown in Figure 2.1 (h), the time evolutions of the strains ($\varepsilon_{horizontal}$ and $\varepsilon_{thickness}$) obtained from experiments and simulations agree very well.

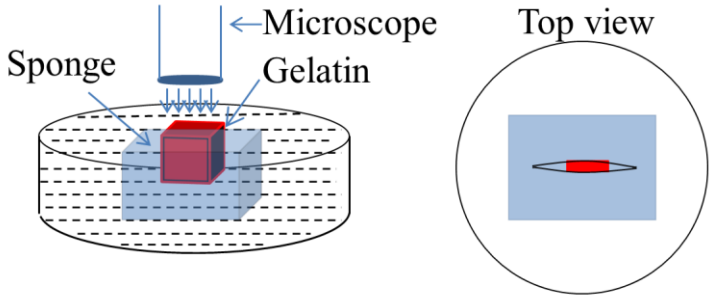

Figure 2.3 Gelatin sheet digestion experiment setup. The gelatin was held vertically by a sponge stage in a glass dish filled with simulated gastric fluid under an optical microscope. The porous sponge was able to keep the gelatin sheet standing in the glass dish and imposed mechanical constraints in the horizontal direction.

A polyelectrolyte drink such as Gatorade (Chicago, IL) with high concentrations of sodium, potassium, citrate, and other stabilizing agents and high ionic conductivity (>2 mS/cm) was used as the electrolyte. Cheese slices (Lucerne Foods, Inc; Pleasanton, CA) were placed between the highly hydrophilic gelatin sheet (package) and gold leaf (current collector) as a segregation layer to avoid direct contact of gelatin and electrolyte. Finally, the package was sealed thermally by an impulse sealer with controlled heat. Thus, an entirely edible supercapacitor was assembled by explicitly using food, including activated charcoal, egg white, gold leaf, roasted seaweed, Gatorade, cheese, and gelatin.

Figure 2.4 (a) presents the cyclic voltammetry (CV) curves of the edible supercapacitor at the scanning rates from 5 mV/s to 100 mV/s. The CV curves are of clearly rectangular shape at lower scanning rates, and become approximately rectangular shape at increased scanning rates, which are ideal for capacitive properties and reversibility of a supercapacitor. The galvanostatic charge/discharge testing result (Figure

2.4 (b)) shows some internal resistance with a constant current density of 1 A/g. After 1,000 charge/discharge cycles (Figure 2.4 (c)), the specific capacitance retains 92.3% by dropping from 78.8 F/g to 72.7 F/g under 1 A/g current density, which is consistent with activated carbon-based supercapacitors (*39*). The degradation mainly results from the electrolyte absorption by the gelatin sheet. To confirm, aluminized polyethylene (PE) (standard packing materials for supercapacitors) and gelatin without cheese segregation have been tested for comparison. The specific capacitance using aluminized PE retains 96.9% by dropping from 76.4 F/g to 74.0 F/g after 1,000 charge/discharge cycles and thus demonstrates excellent electrochemical stability of the electrode-separator-electrolyte system. However, the specific capacitance with gelatin drops more than 50% from 73.2 F/g to less than 34.9 F/g in 100 cycles and to 4.4 F/g in 1,000 cycles. This comparison shows that cheese slices can significantly prevent electrolyte loss and improve the cycling stability. Figure 2.4 (d) presents the electrochemical impedance spectroscopy (EIS) results after one cycle and 1,000 cycles using gelatin sheet with cheese as the packing materials. Only slight resistance increase was observed. Figure 2.4 (e) shows the energy and power densities curve calculated from the constant current density charge–discharge curves measured with 250 mA/g, 500 mA/g, 1 A/g, 2 A/g, and 4 A/g current densities.

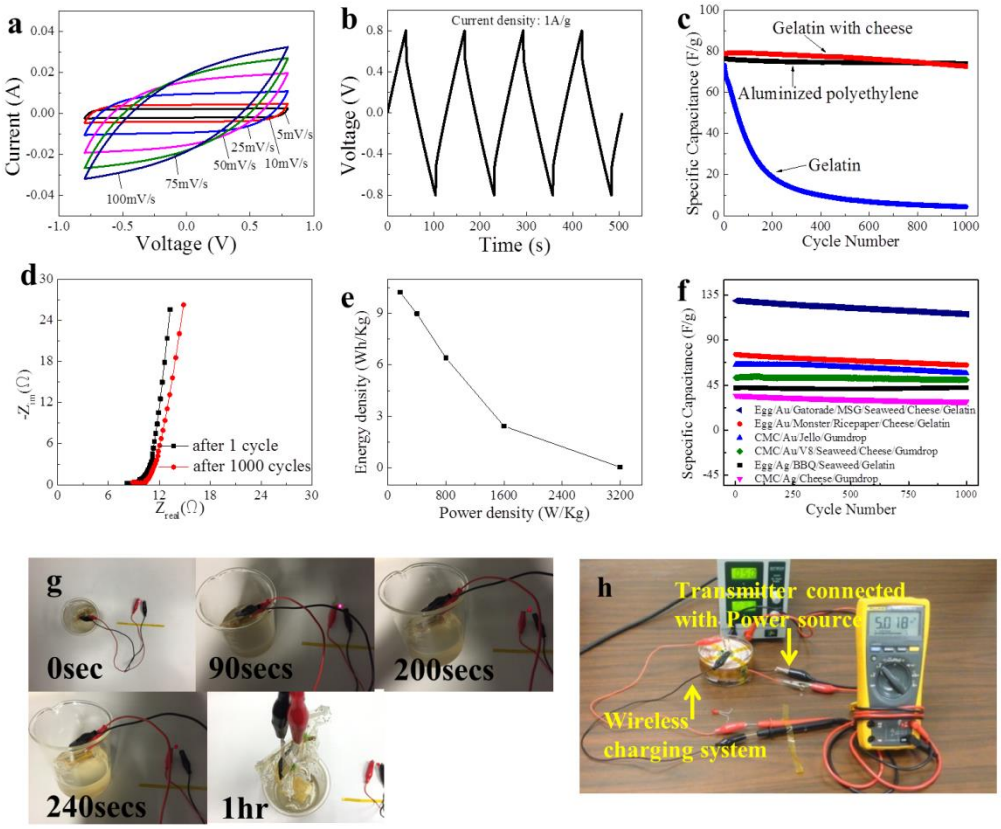

Figure 2.4 Electrochemical characterizations of edible supercapacitors and demonstration of edible supercapacitors powering a LED in simulated gastric fluid. (a) CV curves at the scan rates from 5 mV/s to 100 mV/s. (b-c) Galvanostatic charge-discharge cycles measured with a constant current of 1 A/g, for supercapacitor with gelatin and cheese slides, with aluminized polyethylene (PE), and with gelatin only as package materials. (d) Electrochemical impedance spectroscopy (EIS) analysis before the first discharge cycle and after 1,000 charge-discharge cycles. (d) Energy and power densities calculated from the constant current density charge–discharge curves measured with 250 mA/g, 500 mA/g, 1 A/g, 2 A/g and 4 A/g. (f) 1,000 charge–discharge cycling at a constant current density of 1 A/g for supercapacitors with different materials combinations. (g) Images of supercapacitor set lighting up a LED in simulated gastric solution. (h) The supercapacitor integrated with a receiver coil and AC-DC converting circuit placed in a charging chamber can be wirelessly charged

The material possibilities of edible supercapacitors are immense due to the vast number of available food products. Table 2.1 provides a list of the many other materials investigated including monosodium glutamate (MSG, a flavor enhancer) as electrolyte additive to increase the electrolyte ions density, carboxymethyl cellulose (CMC, a food

additive) as binder, silver leaf as current collector, V8 vegetable drink and Monster Energy drink as liquid electrolytes, BBQ sauce, jello, and cheese as gel electrolytes, and gummy candy as package material. In Figure 2.4 (f), for 1,000 charge-discharge cycles at the current density of 1 A/g, the specific capacitance increases from 78.8 F/g to 129 F/g after the addition of MSG in Gatorade due to the increase of ion densities. The specific capacitances of other liquid electrolytes (V8 vegetable and Monster Energy drinks) show different values due to different ions components and concentrations. Those differences resulted in a difference in conductivity. For example, the conductivity of V8 and Monster Energy drinks are 16.34 μS/cm and 2.18 mS/cm. Due to high internal resistance, the specific capacitances with gel electrolytes (BBQ sauce, jello, and cheese) are lower than those with liquid electrolytes (Figure 2.5). In the following electrochemical characterization, activated charcoal, gold leaf, Gatorade, seaweed, egg white, cheese, and gelatin were used as the model materials for edible supercapacitors.

Table 2.1 Food materials for edible supercapacitors

Binder	**Current Collector**	**Electrolyte**	**Separator**	**Segregation layer**	**Package**
Egg	Au	Gatorade+MSG	Seaweed	Cheese	Gelatin
Egg	Au	Monster drink	Rice Paper	Cheese	Gelatin
CMC	Au	V8 drink	Seaweed	Cheese	Gummy candy
Egg	Ag	BBQ sauce	Seaweed	---	Gelatin

CMC	Au	Jello	---	---	Gummy candy
CMC	Ag	Cheese	---	---	Gummy candy

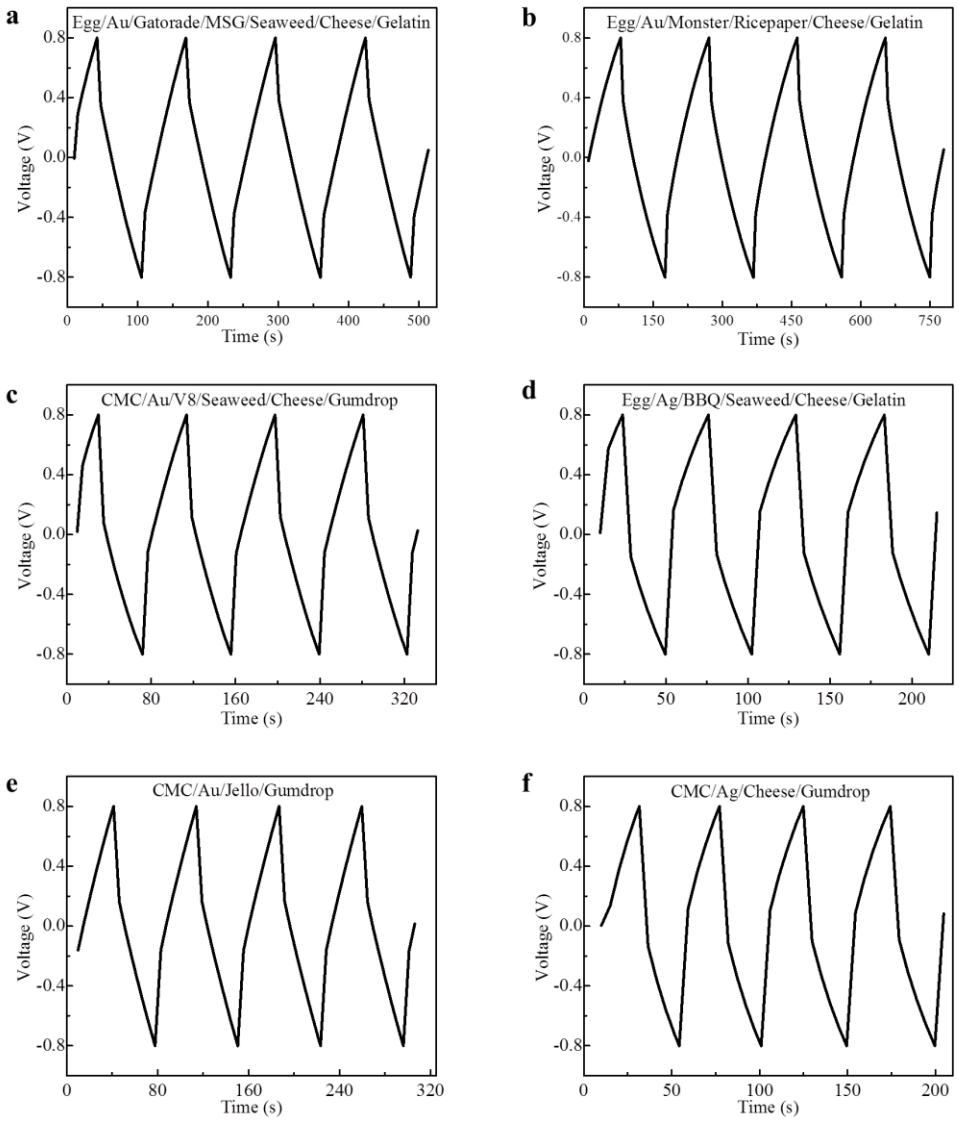

Figure 2.5 Galvanostatic charge-discharge curves for different material combinations at the current density of 1 A/g. The galvanostatic charge-discharge curves for different material combinations at the current density of 1 A/g are shown. For supercapacitors with Gatorade sports drink (a) or Monster energy drink (b) serving as the liquid electrolyte, the internal resistance drop is small compared to those with the V8 vegetable juice (c) or jello (e) electrolyte.

Figure 2.4 (g) demonstrates a supercapacitor set lighting up a light-emitting diode (LED) inside the simulated gastric fluid. The supercapacitor set consists of three supercapacitors (electrode area is 2 cm ×2 cm) connected in series. The LED stayed on for three minutes, followed by gradual dimming and lack of emission after four minutes. After 1 h, the supercapacitor was partially dissolved in the simulated gastric fluid. Figure 2.6 shows the supercapacitor set turning on the LED outside of the fluid. To extend the working time of supercapacitors, a novel wireless charging system was developed (Figure 2.4 (h)). The supercapacitor integrated with a receiver coil and AC-DC converting circuit (GHH, Amazon) placed in a charging chamber can be charged wirelessly in the alternating electromagnetic field (with a frequency of 60 Hz) created by the transmitter coil and DC-AC converting circuit (GHH, Amazon) outside the charging chamber (Figures 2.7-2.9). This novel strategy simulates a scenario where a supercapacitor is inside a human body while it can be wirelessly charged in an alternating electromagnetic field that surrounds the human body.

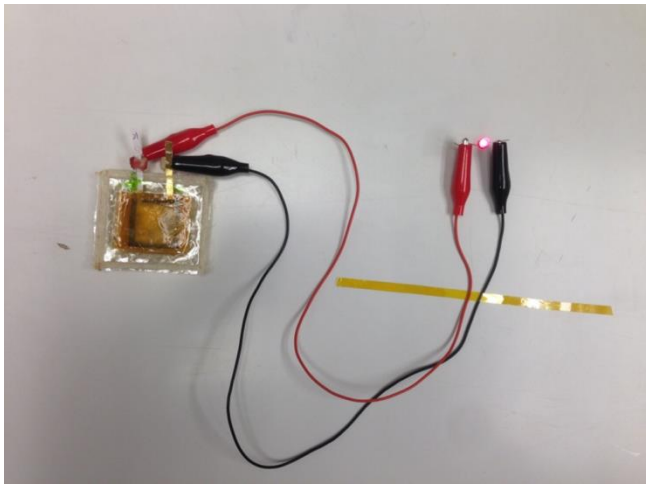

Figure 2.6 Edible supercapacitor lighting up the LED outside of gastric fluid. The LED stays lit for about 10 minutes

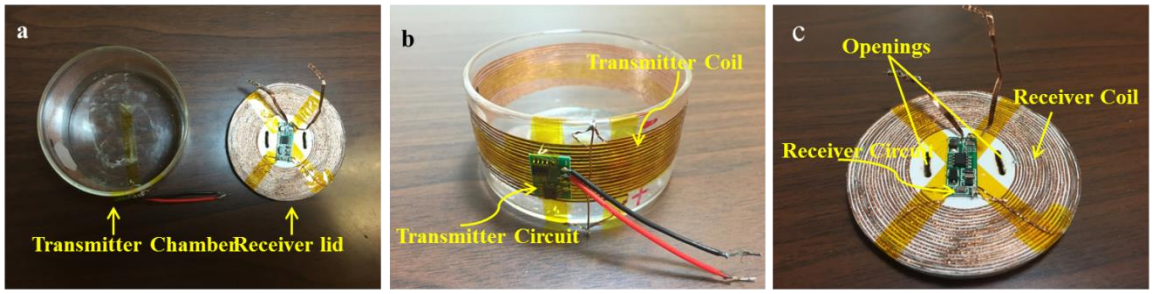

Figure 2.7 Wireless charging system. (a) Top view of wireless charging system, consisting of a transmitter chamber and a receiver lid. (b) Transmitter chamber consists of transmitter coil and circuit on the outside wall of a glass tube. (c) Receiver lid consists of receiver circuit and receiver coil on the surface of a cicular lid made of rice paper and copy paper.

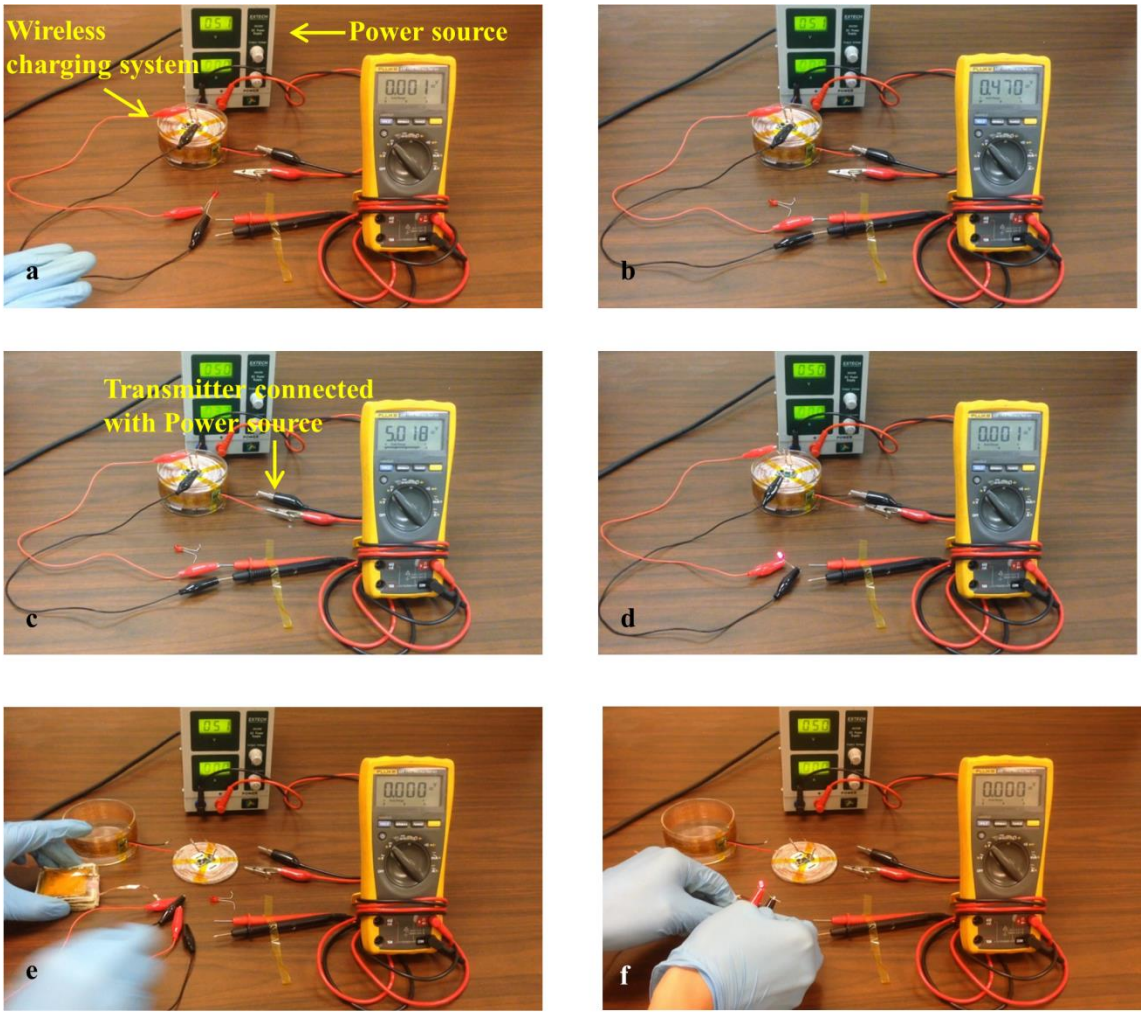

Figure 2.8 Edible supercapacitor charged in a wireless charging system. (a) The setup consists of a constant voltage power source, wireless charging system, LED, and voltage meter. (b) The initial voltage of the supercapacitor set is 0.470 V. (c) The voltage of the supercapacitor set increases to 5.018V. (d) The supercapacitor set lights up a LED inside the charging chamber while the external power source is still wirelessly charging the supercapacitor. (e) The supercapacitor set is removed. (f) The supercapacitor set lights up a LED outside of the charging chamber.

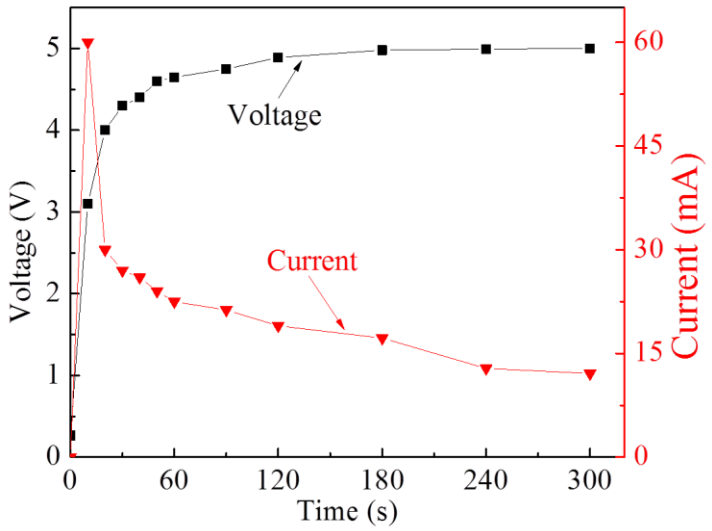

Figure 2.9 Edible supercapacitor current and voltage profiles during wireless charging. With 5.144 V constant voltage output from the receiver, the voltage of the supercapacitor set increases from 0.470 to 4.994 V, and the current decreases from 60 (measured at 10s) to 14.41 mA in 3 minutes. After five minutes, the voltage increases to 5.002 V while the current drops to 12 mA.

The antibacterial activity of electric current has previously been demonstrated against planktonic *Escherichia coli*, *Klebsiella pneumoniae*, and *Proteus* species in various liquids including synthetic urine, water, and salt solutions (*40-44*). Moreover, low-intensity electric current reduced the numbers of viable bacteria in staphylococcal and *Pseudomonas* biofilms after prolonged exposure (1 to 7 days) (*45*, *46*). However, thus far, no real device that can be taken into human body and used to kill bacteria via low-intensity electric current. Here, to further assess potential biomedical applications of the edible supercapacitor, the effect of edible supercapacitor-discharged electric current on bacterial viability was investigated using *E. coli* ATCC 25922 in broth antimicrobial susceptibility experiments. Figure 2.10 (a) presents the edible supercapacitor packaged in standard 000 size gelatin capsule. Figure 2.10 (b) shows two brass rods with stopper

inserted into a 3 mL *E. coli*-PBS suspension. The electric current loop was formed by connecting the outside ends of the rods with the supercapacitor (Figure 2.11). Exponential-phase *E. coli* cells (~10^7 CFU/mL) were resuspended in phosphate-buffered saline (PBS) and exposed to alternating on (2 min) and off (2 min) cycles of electrical current for 60 min. Compared to no electrical current (growth control), a significant reduction ($P < 0.01$) was detected in the number of viable cells present after exposure to supercapacitor-mediated electrical current for 60 min (Figure 2.10 (c)). A time-dependent reduction in bacterial viability was observed, with generally lower viable cell counts detected when electrical current was applied for longer periods of time. The edible supercapacitor causes significant bactericidal activity reduction (99.93% average reduction) after 60 min of alternating on-off current exposures (Figure 2.10(c)). When the replicate experiments were separated based on amperage readings, a higher amperage correlated with a greater reduction in bacterial viability at all time points (Figure 2.10 (d)-(f)), suggesting that proper design of edible supercapacitors better controls the efficiency of antibacterial activity.

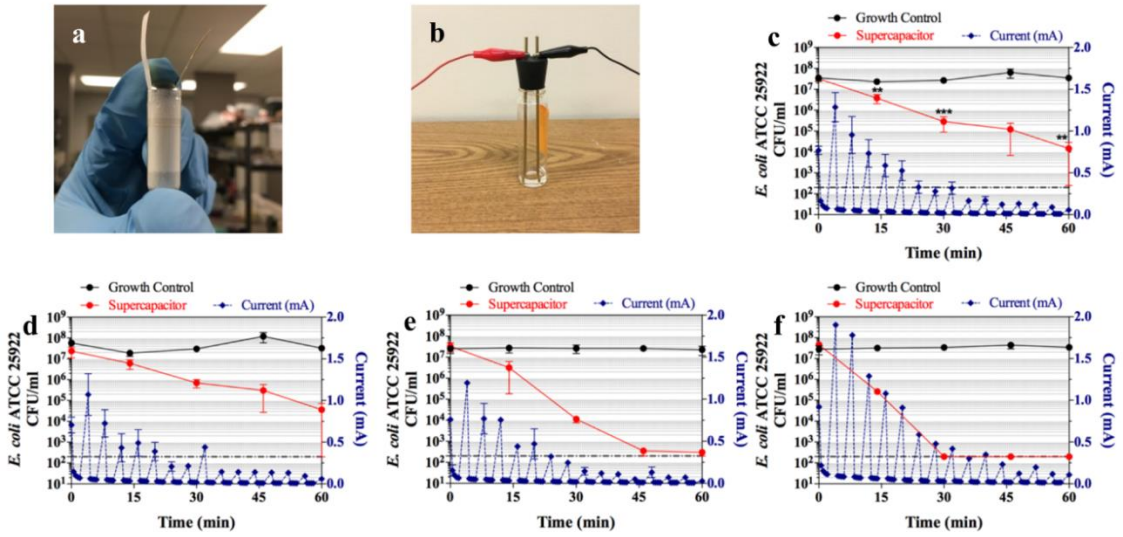

Figure 2.10 *E. coli* survival upon exposure to supercapacitor-mediated electrical current. (a) Image of an edible supercapacitor packaged in a standard 000 size capsule. (b) Image of two brass rods stabilized with a rubber stopper and inserted into the 3 mL *E. coli*-PBS suspension. (c) Exponential-phase *E. coli* was exposed to alternating on-off supercapacitor-mediated electrical current for 60 min. Values represent the mean colony-forming units (CFU) and standard error of the mean (SEM) of five independent experiments. Average current (mA) measurements and SEM of the five independent experiments are shown on the right *y* axis. Correlation (r = 0.9934) between electrical current and bacterial viability for the five independent experiments was determined using Pearson unpaired correlation coefficient. **, $P < 0.01$; ***, $P < 0.001$; unpaired *t* test with Holm-Sidak multiple comparisons. Results of replicate experiments (d, e) or a single experiment (f) with varying supercapacitor currents demonstrate that increasing low-intensity amperage correlates with greater reductions in bacterial viability (r = 0.9673, r = 0.9969, and r = 0.9960, respectively). The detection limit (hatched line) for all experiments was 200 CFU/ml.

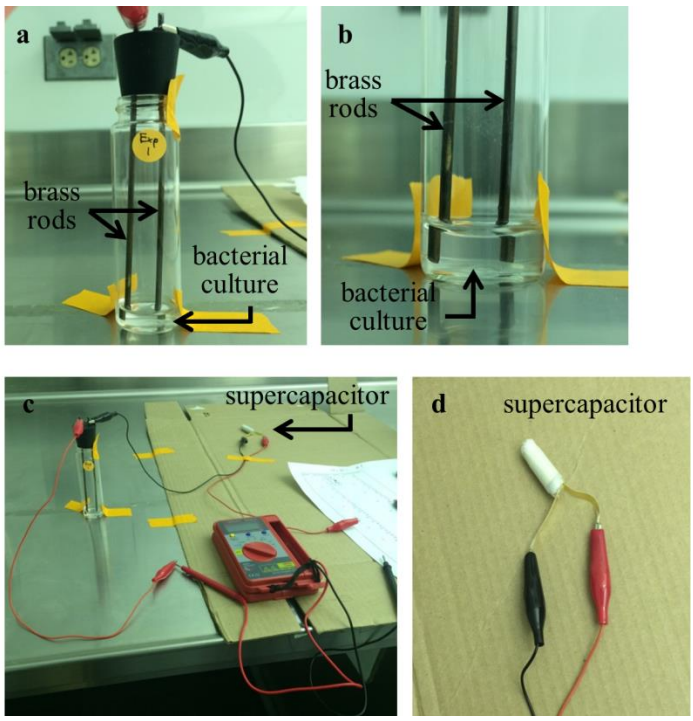

Figure 2.11 Experimental setup for testing antibacterial activity of the edible supercapacitor. (a, b) The current travels through the medium via the brass rods. The bacterial culture consists of *E. coli* (~10^7 CFU/ml) resuspended in 3 mL of PBS. (c) The brass rods in the experimental tube were secured by a rubber stopper and connected to an external edible supercapacitor (d), and the electrical currents were measured simultaneously using jumper wires and a voltage meter. Cardboard was used to insulate the leads from the underlying metal table.

Another promising application of edible supercapacitors is to function as the electrical source for powering an endoscope. Here the edible supercapacitors are able to power a USB endoscope inspection snake tube camera (Silicon_Electronic, Ebay). A USB cable connected to a computer is originally designed for powering the camera and enabling data transmission. To demonstrate our supercapacitors, the positive and negative (ground) power cables of the USB snake camera were cut off and only the data cables were connected to a computer for data transmission (Figure 2.10 (a)). Five fully-charged 4 cm ×4 cm (electrode area) square supercapacitors with an average mass loading of 0.08 g were connected in series to output a 5 V voltage for powering the USB camera that

requires minimum 3.3 V working voltage. The negative terminal of the supercapacitors was connected to the negative (ground) of the snake camera at the beginning to maintain the same reference potential between the computer and supercapacitor. After the positive terminal of the supercapacitors was connected with the positive cable of the snake camera, the camera was recognized and output a 320 × 240 pixels video on the computer screen (Figure 2.10 (b)). The current was measured to be 35 mA. By sweeping the camera back and forth and pointing at the computer screen, the image from the camera was captured and shown on the computer screen. The power cables were then disconnected from the supercapacitors, and one of the supercapacitors was removed and cut open (Figure 2.10 (c)). The cross-section of the opened supercapacitor is shown in Figure 2.12 (d). Finally, the removed supercapacitor was eaten (Figure 2.10 (e)) and swallowed (Figure 2.10 (f)).

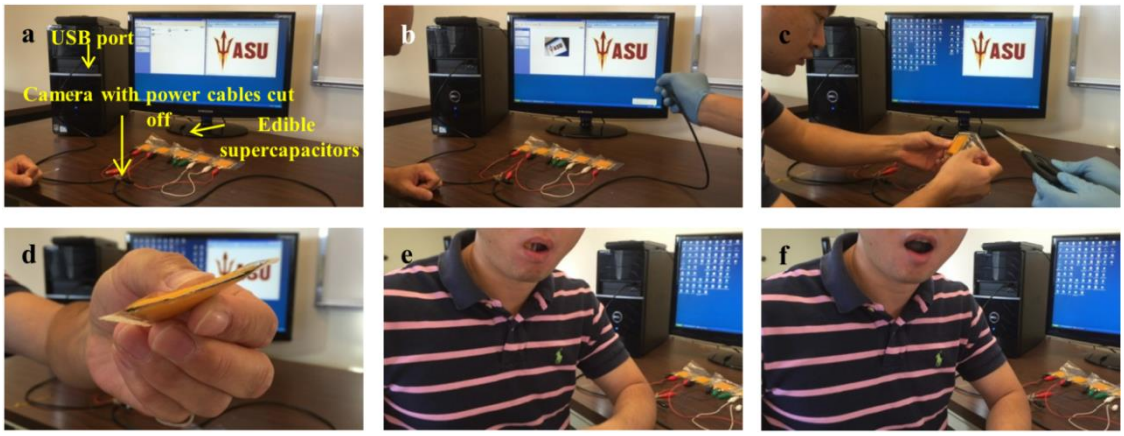

Figure 2.12 Edible supercapacitors powering a snake camera and being eaten. (a) A snake camera with power cables disconnected was plugged in a USB port. Five fully-charged supercapacitors were connected in series to output a 5 V voltage. (b) After the supercapacitor was connected to the USB power cables, the snake camera was recognized and output a video. (c)-(d) A corner of one supercapacitor was cut out. (e)-(f) The removed corner was chewed and swallowed.

CHAPTER 3 EDIBLE ELECTRONICS COMPONENTS

3.1. Background and Motivations

Implantable systems can be more robust, but they are typically more invasive and present a potential risk of infection, bleeding, and a need for surgical recovery in the event of a malfunction. Some of the implantable devices include implantable cardiac devices (*47*), intracranial pressure sensors (*12*), and a swallowable capsule-based devices configured to measure temperature (*11*), pressure (*48*), effectuate imaging (*7, 9*) and measure acidity level (pH) (*10*) data to complement diagnostics and local drug delivery (*49, 50*).

Devices in which the degree of biocompatibility is higher are clearly more preferred as such device are less likely to elicit inflammatory reactions leading, for example, to restenosis in arteries or to tissue scarring in regional implants.

Partially biodegradable electronic devices discussed thus far include a primary battery and biosensor (*14-16, 18*), and an organic field effect transistor (*19, 20*). Notably, completely biodegradable devices still remain a goal, not a reality, primarily due to the lack of biodegradable materials with electrical properties that are comparable to those of available non-degradable metals and insulating materials that are used in conventional passive implantable devices.

Implementations of physically transient electronics have been attempted and include a device that can act as a programmable, non-antibiotic bacteriocide; transient devices (*13, 17*) that incorporate degradable device components, degradable substrates, and/or degradable encapsulating materials; an implantable, tunable, bioresorbable medical

device for nerve stimulation within the body of a patient; and ingestible and/or digestible electronic devices for diagnostic and therapeutic applications. It is well recognized that the results of these initial demonstrations had several significant limitations. One of the practical limitations stems from the fact that the prototypes are typically fabricated using materials that are permanent in shape and/or form and/or substance and largely non-degradable, and thus may require physical retrieval (for example, when these devices have already performed their functions and are no longer required, or in the advent of malfunction). Even if the requirement of or need in retrieval of a given physically transient electronic device is reduced or even eliminated, such device still requires invasive measures for implantation, often via surgery, and thus inherits all usual drawbacks associated with surgery (such as high costs and risks associated with complications that may occur during surgery, after surgery, or both. Another limiting aspect of existing physically transient systems is that - in order to or in attempt to enhance the bioresorbability of such systems and to limit their toxicity and reduce the adverse effects of using such systems - these systems are fabricated with the use of traditional electronics materials but on the geometrically-reduced scale (for example, on a nanoscale) regime in order to enhance their bioresorbablility and limit toxicities and adverse events.

However, these methods require invasive measures for implantation – often via surgery and thus have inherent weaknesses: expensive surgical costs and risks with potential complications that may occur, and more importantly, the use of traditional microelectronics materials as those in the semiconductor area that have limited biocompatibility, toxicity and overall are not “friendly” or safe for the human body. The

search on alternative and friendlier materials that can be used in electronics is emerging. For example, many organic polymers that are used as food additives, such as polyethylene glycol (PEG) and cellulose, was used as emulsifiers and protective coatings in edible electronics (*51, 52*). Silk fibroin was used as flexible substrate, dielectric material or waveguide material (*53*). Among these efforts, edible materials extracted from nature have been explored (*54-56*). These studies, though very limited, initiated a new concept, edible electronics, where the digestive system as a conduit for delivery of electronics that serve as diagnostic and therapeutic tools for the gastrointestinal (GI) system. The potential functions of edible electronics include the basic characterizations of the GI tract, i.e., monitoring of pH, motility, toxins, bacteria, and other vital physiological indicators. The challenge in developing edible electronics is that it is largely unclear if food-based materials are able to provide necessary properties, including electrical properties for the components of the electronics and mechanical properties for the structural integrity.

The present study address the possibility of utilizing basic, largely natural, food materials for the constructs and fabrication of electronic components and devices. The overall hypothesis is that materials derived from natural foods may serve as dominant elements in the fabrication of electronic components and devices and that any gaps in properties not provided by these materials, may be filled in with edible processed foods, food components and on a limited basis non-toxic levels of electronic materials to create full constructs. Best candidate natural, processed and adduct food materials were then selected to create a "preferred food kit" for component fabrication. Specific individual and combined components were built and characterized utilizing the preferred food kit.

3.2. Experimental Section

3.2.1. Preparation of the materials

Dried food: Each vegetable/fruit was cut into round slices with thickness of 1 to 2 mm and diameter of 1 to 4 cm. A household food dryer was used to dry vegetable/fruit slices under 60 ^{o}C for 12 h.

Carbonized cotton candy, cotton and silk: Cotton candy/cotton/silk were annealed at 280 ^{o}C for 1 h at a heating rate of 2 ^{o}C/min, and subsequently annealed at 1000 ^{o}C for 1 h at a heating rate of 6 ^{o}C/min in an argon flow. Then the carbonized cotton candy/cotton/silk were grinded into small pieces (about 300 m in diameter) in a mortar.

Piezoelectric composite thin films: A gelatin/broccoli film worked as piezoelectric film. Gelatin (2 g) was sprinkled over the distilled water (20 g). Leave the mixture for 10 min for the gelatin to fully swell. Then gelatin solution was prepared by dissolving gelatin in distilled water under magnetic stirring for 30 min. The temperature was controlled at 60 ℃. Broccoli powder (0.5 g) and glycerol (1.2 g) were added into gelatin solution and stirred for 10 min. Gelatin/broccoli films were produced by solution casting on acrylic glass plate at 50 ℃ for 12 h.

3.2.2. Preparation of shadow mask

The pattern of the mask was designed in AutoCAD and was transferred into a Mylar film (0.1 mm in thickness) using a laser cutter (VLS 6.60 laser cutter, Universal Laser System, Inc.). The laser cutter would cut through the Mylar film to make a shadow mask.

3.2.3. Preparation of electrical components

(1) Wire/interconnects

The edible wires/interconnects consisted of a substrate and a layer of conductive trace. The substrate was made of rice paper or any other food-based material that has resistivity larger than 1×10^{10} Ω·m. The dimension of rice substrate was 3 mm × (20-50 mm) × 0.2 mm (thickness). A shadow mask with interconnects' pattern was attached to the rice paper using egg white as the adhesive layer. Interconnects were dried in oven at 70 ℃ for 8 h. The substrate was then placed in a vacuum chamber of gold sputtering machine, where gold was deposited on the substrate through the shadow mask, with thickness of 100 nm.

(2) Resistor

Typically, sweet potato starch (1.5 g), active charcoal (0.45 g) and carbonized cotton candy (0.5 g) were mixed together in a ceramic container and grinded for 10 min to make them uniformly dispersed. The container was then put on a hotplate (200 ^{o}C) and heated for 5 min, followed by adding distilled water (2 g) and heating for another 5 min under constant stirring. Now the mixture forms a low-viscous dough. The mixture was then transferred into a syringe. Syringe with different sizes of orifice can be used and in fact the size of the orifice defines the diameter of the edible resistors. The typical diameters are 2 mm. The mixture was pushed out with the rate of 0.7 mL/min into boiled distilled water for 3 min and then immersed in the distilled water of room temperature to make them more tenacity. Finally, the sample was put into an oven and dried at 60 ^{o}C for 12 h. The edible resistors are basically conductive and edible noodles. Carbonized cotton and

silk can be similarly used to replace cotton candy. Flour can also be used to replace sweet potato starch in this process.

(3) Inductor

The edible inductors were made by following the similar procedure of making edible resistors. After the mixture was pushed into the boiled distilled water and immersed in the distilled water of room temperature, the sample was winded around a cylindrical object (e.g., a tube). The winding length and diameter define the inductance. The typical diameters are 2 mm and the length ranges from 40 to 80 cm. Then, they are dried in an oven with 60 ^{o}C for 12 h. Finally, after the sample was completely dried, it was taken off from the cylindrical object.

(4) Capacitor

A gelatin film was used as the dielectric layer. Gelatin (2 g) was sprinkled over the distilled water (20 g). Leave the mixture for 10 min for gelatin to fully swell. Then gelatin solution was prepared by dissolving gelatin in distilled water under magnetic stirring for 30 min. The temperature was controlled at 60 ℃. Glycerol (1.2 g) was added into gelatin solution as plasticizer and stirred for 10 min. Gelatin films were produced by solution casting on acrylic glass plate at 50 ℃ for 12 h. The typical thickness of the gelatin film varies from 80 m to 140 m. The pattern of the metal trace was defined by a shadow mask. Two same shadow masks were attached to gelatin film's both sides with carefully alignment. Gold was deposit for 200 nm thickness on both sides using gold sputter. The shadow masks were removed after deposit and the capacitor was just made.

(5) PCB board

Each edible PCB board substrate consists of powdered sugar, xanthan gum and egg white. Powdered sugar (60 g), xanthan gum (0.5 g) and egg white (12 g) were mixed together in a glass bowl by hand mixer. Keeping mixing them until a sticky paste was achieved and most of the powdered sugar was incorporated. Additional powdered sugar (20 g) and the sticky paste were poured on the workbench. Kneading them until a smooth and non-sticky dough was formed. The sugar paste dough was divided by 8 pieces. Each of them was rolled out and cut into a 7 cm $\times$7 cm $\times$0.2 cm piece, followed by drying at room temperature for 12 hrs. Before placing shadow mask on substrate, a uniform egg white layer was coated on the surface of substrate. Egg white will make the surface adhesive to have a good connection with shadow mask. Substrate will be ready to be deposited gold against a shadow mask after drying it in oven at 70 ℃ for 8 h.

(6) Antenna

The shadow mask is made using the same method described previously. Then the shadow mask is attached to the PCB board substrate, followed by gold deposit using gold sputter for 200 nm. The shadow mask is removed after deposit and the antenna is made.

3.2.4. Preparation of samples for mechanical test

The same procedure was followed to prepare sweet potato starch dough, powdered sugar dough, and flour powder dough. All the dough was kneaded and cut into a plate with dimension of 3 $\times$2 $\times$0.2 cm for the mechanical test. The Instron 4411 was used to perform the compression test.

3.2.5. Characterization of materials, components, and devices

(1) Conductivity characterization

Potentiostats (Gamry Potentiostats Reference 300) and multimeter (hp Hewlett Packard) were used for raw and dried food materials. For powdered food material: A stainless steel mold with 1-inch in diameter was used to hold the powder food material, including fresh milk powder, carbonized cotton candy/cotton/silk, all-purpose flour and sugar powder. Then 30 MPa pressure was applied on the mold to achieve a condensed tablet. Two stainless steel plates were placed on two sides of food material tablet to form a "sandwich" structure for electrical conductivity measurement (Figure 3.1) using Gamry Potentiostats Reference 3000. For liquid food material, a plastic box with copper foils on two sides (Figure 3.2) was used to hold the liquid food material. Then two copper foils were connected to multimeter for the resistance measurement.

Figure 3.1 "Sandwich" structure for electrical conductivity measurement.

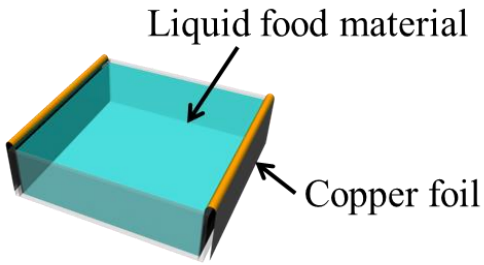

Figure 3.2 Sample holder for electrical conductivity measurement for liquid materials.

(2) Capacitance measurement

It was measured on probe station with precision LCR meter (Hewlett-Packard 4061A semiconductor/component test system).

(3) Inductance measurement

The dimensions are measured with caliper and the inductance was measured by the same equipment for the capacitance measurement.

3.2.6. Mechanical characterization of food materials used as the structural functions

The sample is placed on the platform of the tool material test system (Instron 4411) for compression test. After initial setup, compressive force through a pressing target is loaded and recorded as well as the displacement of the pressing target until failure of the sample. The first few data are used to calculate the Young's Modulus. The stress is calculated by dividing force by top area of the sample, and the strain is calculated by dividing displacement and thickness of the sample. Then the Young's Modulus is calculated by dividing stress by strain.

$$E = \frac{\sigma}{\varepsilon}$$

$$\sigma = \frac{F}{a}$$

$$\varepsilon = \frac{\Delta l}{l}$$

3.2.7. Characterization of the piezoelectric coupling coefficient

(1) d_{33}**:** Sample's dimensions, weight and capacitance were measured before the test. The schematic of the characterization is shown in Figure 3.3, where a beam was

fixed at an end and the other end was attached to an electric shaker. The sample was attached onto the beam at the 3/4 of distance to the end of the shaker by wax and an accelerometer was mounted at the same location to measure the acceleration of the sample. The electric shaker was connected to its power supply and a signal generator with frequency of 50 Hz. During the vibration applied by the shaker, the inertia force was applied to the sample via F = ma, which generates a voltage V at the sample that was characterized by a signal analyzer. Thus the piezoelectric coefficient d_{33} is calculated by $d_{33} = \frac{CV}{F}$, where C is the capacitance of the sample that was characterized separately.

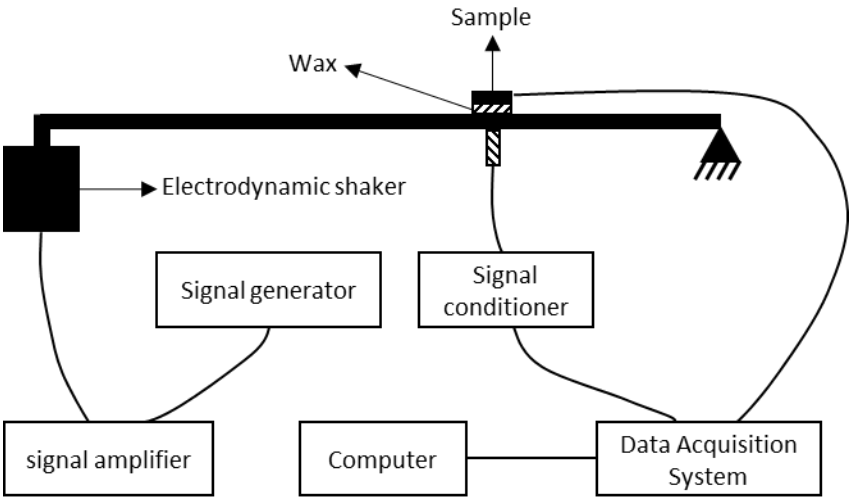

Figure 3.3 Schematic of the characterization of d_{33}.

(2) d_{31}: D31 was characterized by a fatigue load frame (Bose ElectroForce Biodynamic 5160) and current was measured with a picoammeter (Keithley 6485) (Figure 3.4 (a)). The samples were prepared with 8×25.4mm Ag paint electrodes in top and bottom surfaces, and the electrodes were then extended with Cu tape to allow a

proper connection with the picoammeter (Figure 3.4 (b)). Dynamic force was applied on the sample to measure periodic output current.

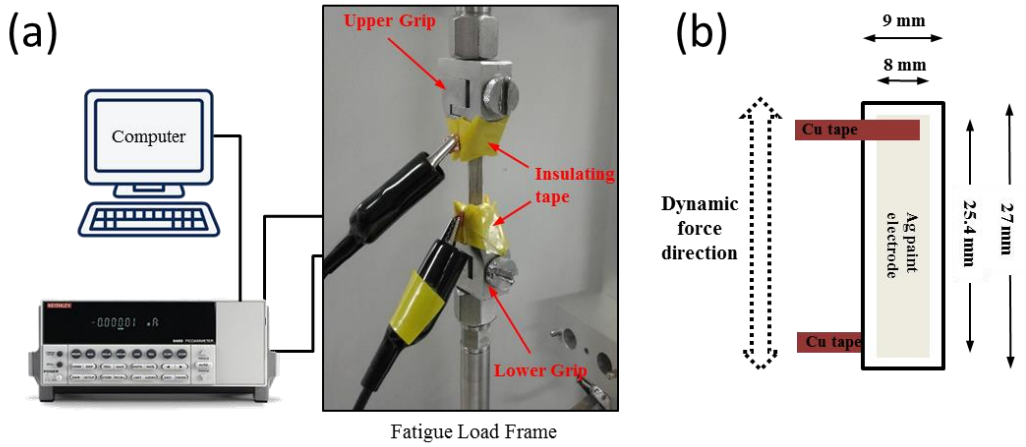

Figure 3.4 (a) Equipmental set up for characterization of d_{31}. (b) Sample and electrode design.

3.2.8. **Field Scanning electron microscopy (FESEM)** and **Energy dispersive X-ray spectrometry (EDX) Test**

The surface morphology and element content of carbonized cotton candy/cotton/silk, broccoli powder, piezoelectric film, inductor and conductor were observed using scanning electron microscopy (Hitachi S4700 FESEM). Broccoli powder and piezoelectric film were coated with 200nm gold in a vacuum chamber of gold sputter machine before taking SEM. EDX of activated charcoal and carbonized cotton candy/cotton/silk were taken in the same instrument (Hitachi S4700 FESEM).

3.3. Result and discussion

In the present study, natural foods and foodstuffs were chosen as candidates for electronics materials and then based on specification requirements identified additional

edible processed foods, food components, and on a limited basis nontoxic levels of electronic materials, to create full electronic constructs. The best candidates from natural, processed, and adduct food materials were then selected to create the "preferred food kit" for component fabrication. Specific individual and combined components were built and characterized utilizing the preferred food kit. The present study significantly enables edible electronics with the potential to advance an emerging domain of biomedical technologies and devices.

As a first step, reference materials were selected to establish the specifications needed for components. Electronic components require insulators and conductors, which can be specified by their electrical conductivities. For insulators (or dielectric materials), the conductivity needs to be lower than 10^{-8} S/m; while it needs to be larger than 10^{6} S/m for conductors. (*59*) The insulators are used to build encapsulations and as the dielectric materials in capacitors with the capacitance in the typical range of 1 pF-100 nF. (*60*) The conductors appear in wires/interconnects, electrodes and other components. Mixed insulators and conductors can be used to build resistors with a wide range of resistance from 10 Ω-20 MΩ. (*60*) Those reference values establish the specifications needed for components and devices fabrications using food materials.

As a second step, specific natural, unprocessed foods were selected, organized according to recognized, defined nutritional food groups from the Food Guide Pyramid (e.g., cereals, meat, vegetables, bread, fats, etc.), as candidate materials for analysis due to their electrical properties and subsequent component or device fabrication. Conductivity probes and semiconductor parameter analyzer were used to perform the characterizations (see details in Methods). As seen in Figure 3.5 (a) for electronic

conductivities, oils and dried foods (including meat, vegetables, gelatin, fruits, and bread) that are shaded achieve required conductivities as insulators/dielectric materials. Here gelatin was cataloged into meat as it is derived from collagen in animal raw materials. The dried foods were made using a typical food dryer. The reason of being good insulators is that those foods are covalent components (*59*) and do not contain mobile electrons to conduct electric current. On the contrary, foods that contain salts (e.g., butter) and water (e.g., fresh meat and vegetables) are relatively conductive because of the presents of free ions to conduct electric current. A more comprehensive list of electrical conductivity and dielectric constants of commonly accessible food materials were provided in Table 3.1. Figure 3.5 (a) apparently shows that nature foods can provide good insulators/dielectric materials but not good conductors for electrical components.

In order to fill the gap in conductivity to create full constructs in electronic components, processed foods and non-toxic levels of electronic materials were identified. In addition to edible metals as conductors, carbon derived from processed foods, basically activated charcoal, carbonized sugar (cotton candy), cellulous (cotton), and protein (silk) were selected and tested. Annealing process was used for carbonization (see Methods). The energy dispersive X-ray spectrometry (EDX) results show that they are actually carbon. (see Figure 3.6). Different microscale morphologies of carbonized cotton candy (Figure 3.5 (b)), cotton (Figure 3.5 (c)), and silk (Figure 3.5 (d)) as observed in the scanning electron microscope images attribute to different electrical properties. Specifically, the fiber-liked carbonized cotton tends to form a continuous path to conduct electron while the flake-liked carbonized cotton candy and silk have to aggregate to form the similar conductive path. The electronical conductivity results given in Table 3.2 show

that these processed food materials and non-toxic metals can serve as the conductive materials. It is apparent from Figures 3.5 (a)-(d) and Table 3.1 and 3.2 that edible food materials can cover a wide range of electrical conductivity as shown in the conductivity spectrum Figure 3.5 (e). To build a conductive wire/interconnect, edible metals are good choices while dried vegetables mixed with bread/flour and oil are good candidates for insulators. The mixed carbonized cotton candy and flour can be used to build resistors.

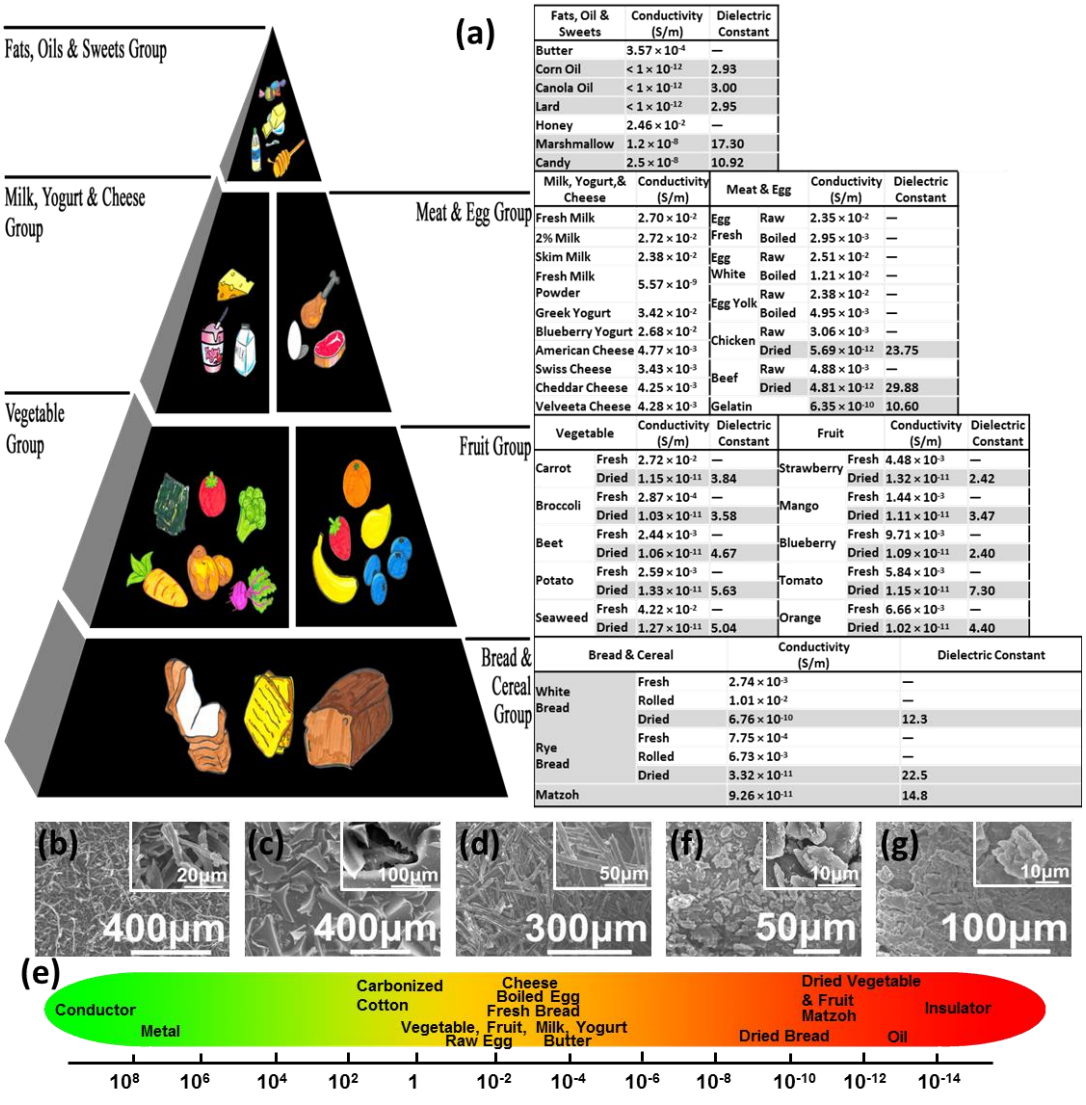

Fats, Oil & Sweets	Conductivity (S/m)	Dielectric Constant
Butter	3.57×10^{-4}	—
Corn Oil	$<1\times10^{-12}$	2.93
Canola Oil	$<1\times10^{-12}$	3.00
Lard	$<1\times10^{-12}$	2.95
Honey	2.46×10^{-2}	—
Marshmallow	1.2×10^{-8}	17.30
Candy	2.5×10^{-8}	10.92

Milk, Yogurt,& Cheese	Conductivity (S/m)
Fresh Milk	2.70×10^{-2}
2% Milk	2.72×10^{-2}
Skim Milk	2.38×10^{-2}
Fresh Milk Powder	5.57×10^{-9}
Greek Yogurt	3.42×10^{-2}
Blueberry Yogurt	2.68×10^{-2}
American Cheese	4.77×10^{-3}
Swiss Cheese	3.43×10^{-3}
Cheddar Cheese	4.25×10^{-3}
Velveeta Cheese	4.28×10^{-3}

Meat & Egg		Conductivity (S/m)	Dielectric Constant
Egg Fresh	Raw	2.35×10^{-2}	—
	Boiled	2.95×10^{-3}	—
Egg White	Raw	2.51×10^{-2}	—
	Boiled	1.21×10^{-2}	—
Egg Yolk	Raw	2.38×10^{-2}	—
	Boiled	4.95×10^{-3}	—
Chicken	Raw	3.06×10^{-3}	—
	Dried	5.69×10^{-12}	23.75
Beef	Raw	4.88×10^{-3}	—
	Dried	4.81×10^{-12}	29.88
Gelatin		6.35×10^{-10}	10.60

Vegetable		Conductivity (S/m)	Dielectric Constant
Carrot	Fresh	2.72×10^{-2}	—
	Dried	1.15×10^{-11}	3.84
Broccoli	Fresh	2.87×10^{-4}	—
	Dried	1.03×10^{-11}	3.58
Beet	Fresh	2.44×10^{-3}	—
	Dried	1.06×10^{-11}	4.67
Potato	Fresh	2.59×10^{-3}	—
	Dried	1.33×10^{-11}	5.63
Seaweed	Fresh	4.22×10^{-2}	—
	Dried	1.27×10^{-11}	5.04

Fruit		Conductivity (S/m)	Dielectric Constant
Strawberry	Fresh	4.48×10^{-3}	—
	Dried	1.32×10^{-11}	2.42
Mango	Fresh	1.44×10^{-3}	—
	Dried	1.11×10^{-11}	3.47
Blueberry	Fresh	9.71×10^{-3}	—
	Dried	1.09×10^{-11}	2.40
Tomato	Fresh	5.84×10^{-3}	—
	Dried	1.15×10^{-11}	7.30
Orange	Fresh	6.66×10^{-3}	—
	Dried	1.02×10^{-11}	4.40

Bread & Cereal		Conductivity (S/m)	Dielectric Constant
White Bread	Fresh	2.74×10^{-3}	—
	Rolled	1.01×10^{-2}	—
	Dried	6.76×10^{-10}	12.3
Rye Bread	Fresh	7.75×10^{-4}	—
	Rolled	6.73×10^{-3}	—
	Dried	3.32×10^{-11}	22.5
Matzoh		9.26×10^{-11}	14.8

Figure 3.5 Selections and characterizations of food-based materials regarding their electronical properties. (a) A typical food pyramid with conductivities and dielectric constants of some representative food materials according to recognized food groups. The

shaded elements represent food materials that can provide required conductivities as insulators/dielectric materials. (b)-(d) Scanning electron microscope (SEM) images for carbonized cotton candy, cotton, and silk, respectively. (e) Conductivity spectrum of food-based materials that can cover a wide range of electrical conductivity from conductors to insulators. (f)-(g) SEM images for broccoli powder and the cross-sectional view of the edible piezoelectric thin film consisting of gelatin and broccoli powder.

Table 3.1 Comprehensive list of conductivity of commonly accessible food materials

Food materials		**Conductivity (S/m)**	**Dielectric Constant**
Fats, Oil & Sweets	Gummy Bears	5.78×10^{-5}	—
	Chewing Gum	4.79×10^{-8}	23.10
	Sugar	2.58×10^{-9}	9.53
	Glucose	1.01×10^{-9}	4.78
	Dextrose	1.40×10^{-9}	5.26
	Molasses	7.14×10^{-4}	—
	Karo Syrup	1.25×10^{-3}	—
Meat & Egg	Chicken (Cooked)	9.43×10^{-4}	—
	Beef (Cooked)	4.74×10^{-4}	—
Vegetable	Guar Gum	5.2×10^{-9}	9.99
	Xanthan Gum	8.43×10^{-10}	16.30

	Kale (Fresh)	6.42×10^{-6}	—
	Kale (Dry)	2.25×10^{-11}	6.58
	Cauliflower(Fresh)	3.11×10^{-5}	—
	Cauliflower (Dry)	2.04×10^{-11}	4.97
	Cucumber (Fresh)	8.83×10^{-4}	—
	Cucumber (Dry)	0.86×10^{-11}	5.37
Fruit	Banana (Fresh)	4.79×10^{-3}	—
	Banana (Dry)	1.12×10^{-11}	6.00
	Pineapple (Fresh)	1.75×10^{-3}	—
	Pineapple (Dry)	1.38×10^{-11}	4.56
	Avocado	2.48×10^{-3}	—
Bread & Cereal	Flour	5.67×10^{-10}	6.32
	Corn Starch	2.93×10^{-10}	7.95

Table 3.2 Conductivity of processed food materials

Processed Food	**Conductivity (S/m)**
Carbonized Cotton	35.07

Carbonized Cotton Candy	22.46
Carbonized Silk	28.29

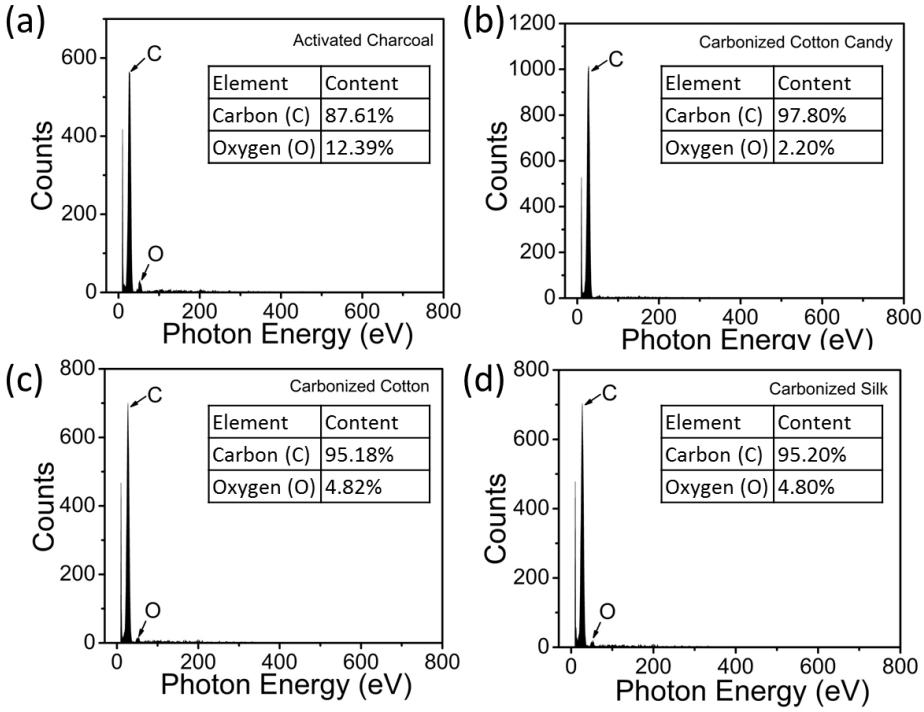

Figure 3.6 EDX test result of (a) activated charcoal, (b) carbonized cotton candy, (c) carbonized cotton, and (d) carbonized silk.

In addition to insulators and conductors in electrical components, other functional materials are also indispensable, particularly for sensing. For example, piezoelectric materials can generate electricity upon mechanical stress and have been used in many applications including pressure sensors, microphones and speakers. Many nature and edible materials have piezoelectric effects, such as bones and tendons (*61-63*). Cellulose that is rich in many vegetables (such as broccoli and brussels sprouts) also has piezoelectric effects. The mechanism is that the oriented cellulose crystallites in these

vegetables exhibit shear piezoelectricity due to the internal rotation of polar atomic groups associated with asymmetric carbon atoms (*64*). Here broccoli powder with radius less than 90 m was used to mix with gelatin to form a piezoelectric composite. SEM images show the broccoli powder (Figure 3.5 (f)) and a cross-sectional view of the edible piezoelectric thin film (Figure 3.5 (g)). Broccoli powders (Holistic Herbal Solutions, LLC) were sieved through a sieve with mesh size 90 m and they uniformly mixed with gelatin solution through magnetic stirring followed by casting under room temperature. The stiffness of the thin film can be tuned by adding edible plasticizer glycerol (see Methods). The piezoelectric coupling coefficients of the edible piezoelectric thin film were characterized by using electric shaker, accelerometer and signal analyzer (see Methods). They are d_{33} = 4.3 pC/N, and d_{31} = 0.31 pC/N. These values are comparable to 5 pC/N of ZnO (*65, 66*). In addition to broccoli that is rich in cellulous, other cellulous-rich foods, including brussels sprout and cabbage were also mixed with gelation to form piezoelectric composites using the similar approach. The same characterization approach was used and the results are given in the Fig 3.7. It is concluded that they all exhibit appreciable piezoelectric effects. Under the same weight ratio between cellulous-containing vegetables and gelatin, broccoli has the strongest piezoelectric effects since it is the most cellulous-rich vegetables (*67, 68*). It should be noted that gelatin also has detectable piezoelectric effects since it is derived from collagen in animal raw materials. However, its d_{33} is about 30 times less than that of broccoli (Table 3.3).

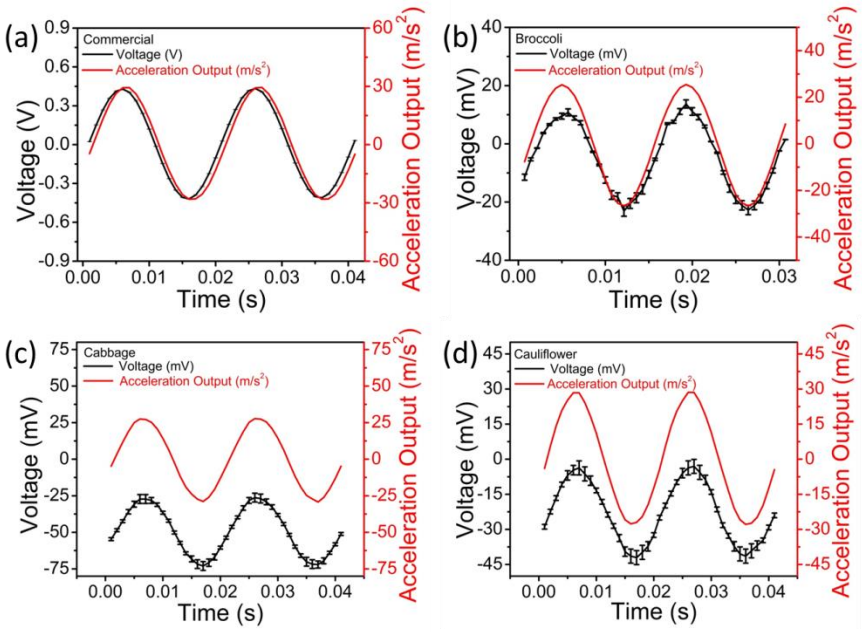

Figure 3.7 Characterization of the piezoelectric performance of (a) commercial PZT film and films which were made with (b) broccoli, (c) cabbage and (d) cauliflower. Besides broccoli/gelatin piezoelectric thin films, cabbage and cauliflower as the active materials in the piezoelectric thin films are also made using the same procedures.

Table 3.3 D33 of different piezoelectric materials

Piezoelectric materials	**D33 (pC/N)**
Commercial PZT	550
Pure gelatin film	0.185
Broccoli/gelatin film	4.30
Cabbage/gelatin film	0.66
Cauliflower/gelatin film	3.00

The studies of food materials with respect to their electrical properties opens opportunities to build a toolkit for necessary electrical components, as shown in Table 3.4. The food materials in the toolkit are grouped into structural and electrical functions. Insulative food materials, such as sweet potato starch, sugar powder, and flour, basically provide structural functions. Distinct applications of these materials in electrical components attribute to their different mechanical properties (e.g., elastic modulus and bending rigidity). The characterization approach is in Methods and their mechanical properties are in the Supporting Information. Specifically, rice paper is very thin and thus very flexible so that it is used as the substrate in wires/interconnects. Though both sweet potato starch and flour can be used as the substrate in resistors and inductors, a dough of sweet potato starch is easy shaped and tends not to fracture at the dried state, compared with regular flour. The reason is that sweet potato starch contains more starch than flour, and starch will gelatinize in the presence of water and heat. After gelatinization, starch dough will become uniform and sticky which makes it easy to be shaped into desired shapes with smooth surface. Thus sweet potato starch can serve as a good substrate for resistors and inductors. The conductive food materials, such as edible metals and carbonized cotton candy, contribute to the electrical functions. The wires/interconnects need to have very small electrical resistance so that edible metals are used; while for resistors, carbonized cotton and cotton candy that have relatively low electrical conductivity are used. To achieve good adhesive between the substrate and conductive regions, egg white was used as the binding materials if necessary. The presence of hydrogen bonds and ionic interactions with proteins attribute high adhesive strength and allows egg whites as good adhesive materials.

The components in Table 3.4 were built using the suggested food materials. The optical microscopy and SEM images along with the characterization results are shown in Figures 3.8. The detailed fabrication approaches are in Methods and characterizations in Supporting Information with a brief description here. The edible wires are made of rice paper as the substrate and sputtered Au as the functional part. The thickness of the Au is on the order of 100 nm (Figure 3.8 (a)). The resistors and inductors are all made of sweet potato starch and carbonized cotton candy through an extrusion process using a syringe, where the resistors are straight wires (or basically conductive “noodles”) and the inductors are winded against a cylindrical object (or basically noddle-based spring). Another layer of carbonized cotton was added on the outside of the noodles while they are still wet to increase the conductivity. As shown in the SEM images in Figure 3.8(b), carbonized cotton forms a continuous path in the noodles. The capacitors are made of thin gelatin sheets as the dielectric layers coated with edible Au as the electrodes. The thickness of the gelatin is in the range of 80 m to 140 m (Figure 3.8 (d)). By adding glycerol as the plasticizer and also a high-k material in gelatin, the mechanical flexibility and effective dielectric constants can be improved. A plasticizer could reduce the glass transition temperature (Tg) and increase the plasticity of the material. Glycerol as a common plasticizer are widely used in the pharmaceutical field, such as softening the capsule and biomedical or biodegradable materials.In addition to the food materials presented in Figures 3.8, more food materials have been used to build these components. Similar characteristics have been achieved as shown in the Figure 3.9-3.12. It is thus convincing that edible food materials are able to build functional circuits.

Table 3.4 A toolkit using food-based materials to build necessary electrical components.

Component	Food Kit Materials	
	Structural Function	**Electrical Function**
Wire	Rice paper, sugar powder, wheat flour, rice	Gold leaf, edible metal: gold
Resistor	Sweet potato, sugar powder, wheat flour, hard candy, dried fruit, vegetable	Active charcoal, carbonized cotton fiber / cotton candy / silk, gold leaf
Inductor	Sweet potato powder, wheat flour, hard candy, dried fruit, dried vegetable	Active charcoal, carbonized cotton fiber / cotton candy / silk, gold leaf
Capacitor	Gelatin, dried fruit, dried Vegetable	Gold leaf, edible metal: gold
Antenna	Sugar powder, wheat flour, rice paper, hard candy, marshmallow, egg white	Edible metal: gold, gold leaf, active charcoal, carbonized cotton /silk

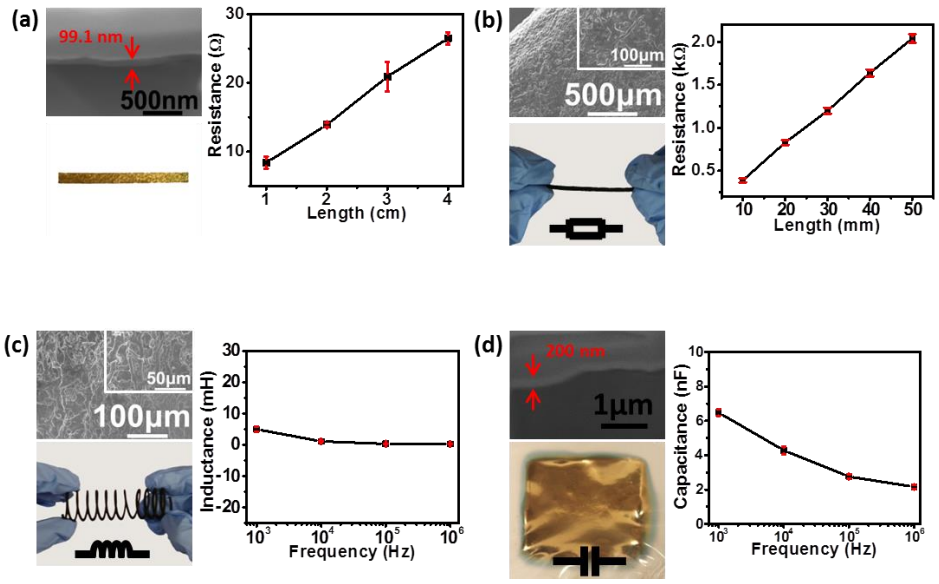

Figure 3.8 Results of food-based electrical components. Optical and SEM images are shown, along with the characteristics of the components. (a) Wires; (b) Resistors; (c) Inductors; (d) Capacitors.

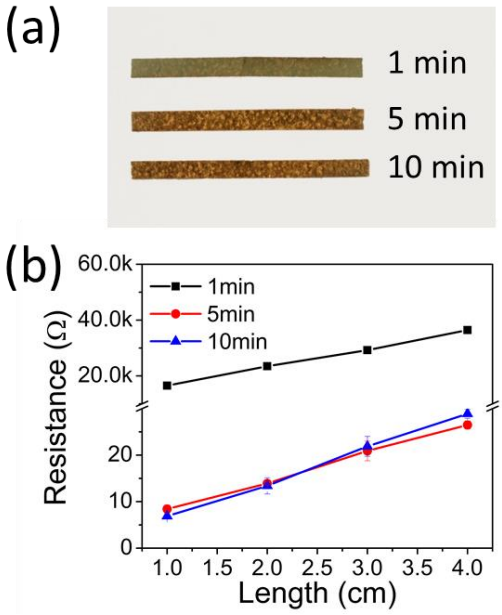

Figure 3.9 (a) Images of wires with different Au coating time, 1, 5 and 10 mins. (b) Resistance test result of wires with different coating time.

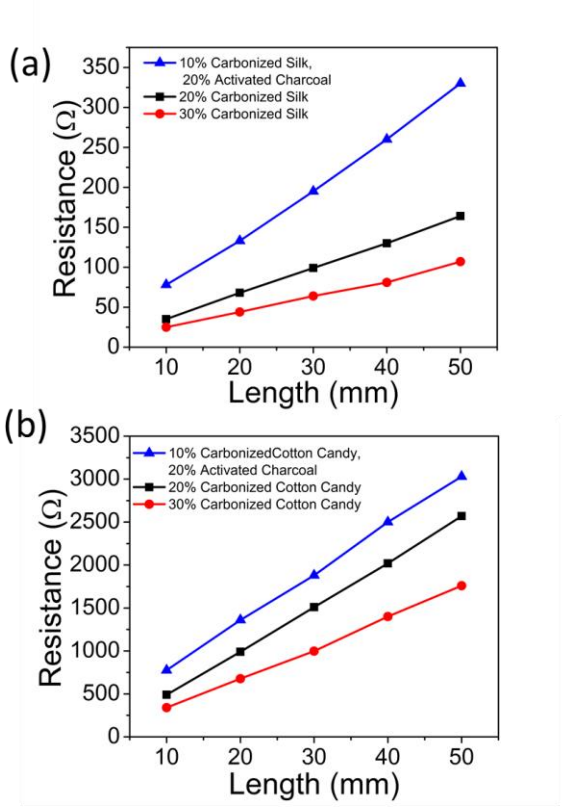

Figure 3.10 Resistance test result of resistors with different composites. Resistors with different composites were made to get a wide range of resistance. Carbonized silk and carbonized cotton candy were used as a substitute for carbonized cotton. The content of carbonized silk and carbonized cotton candy was controlled at 10%, 20% and 30%.

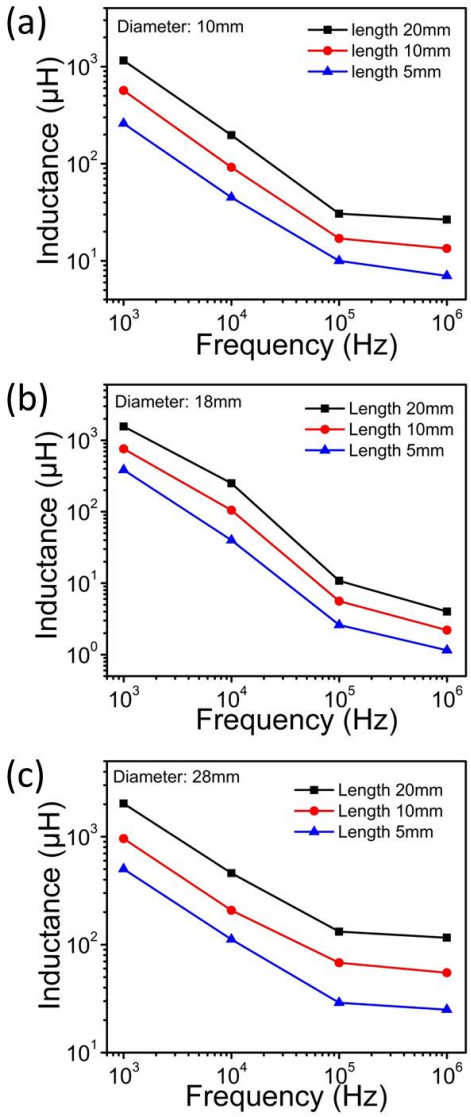

Figure 3.11 Performance of inductors with different diameters under frequency range from 10^3 to 10^6 Hz.

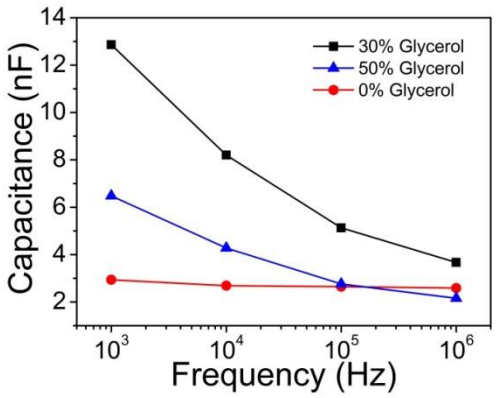

Figure 3.12 Properties of capacitors with different composition under frequency range from 10^3 to 10^6 Hz.

CHAPTER 4 EDIBLE PH SENSORS

4.1. Background and Motivation

In the previous chapter, a new class of electronic materials derived predominantly from natural foods and foodstuffs, with minimal levels of inorganic materials, is developed and studied to build edible electronic components. Edible electronic components can be further integrated into edible systems and devices which can function as comparable electronics.

On-person electronics, as either wearable or implantable systems, have an increasingly significant role in healthcare monitoring, diagnosis and therapy. Progress in the development of healthcare devices has been boosted by dramatic advances in electronic materials - with expansion of the form factor and constituents of electronic materials as well as with the advent of flexible, stretchable, and transient systems. Skin-based systems are able to detect variables such as heart rate (*69, 70*), temperature (*71, 72*), and sweat-based body constituents (*73, 74*). Implantable systems can be more robust, but they are invasive and present a risk of infection, bleeding, and a need for surgical recovery in the event of a malfunction.

One body domain that has only been partially explored to administer electronics has been the gastrointestinal (GI) tract. The GI tract is a primary interface between the external environment and the internal milieu, affording tremendous surface area for device residence and monitoring of a wide range of health and disease conditions and states. To date a limited number of devices have been fabricated for GI use. These devices may, for example, be swallowed whole or implanted via endoscopy.

These include capsule endoscopes (PillCam™, Medtronic, Minneapolis, MN) and capsules to measure GI motility (*75, 76*) and pH (*76, 77*)(SmartPill™, Medtronic, Minneapolis, MN). These devices are not biodegradable and run the risk of causing bowel obstructions if they become entrapped in areas of stenosis. They are also relatively expensive. For these reasons they are not suitable for repeated administration over time. Acid peptic disorders are extremely common and are treated with acid suppression medications that carry risk. There is a critical need to be able to measure gastric pH repeatedly over time to diagnose these disorders, objectively monitor response to therapy in order to use the lowest effective dose of medicine, and in a safer and more cost-effective manner than currently available.

Currently, to measure gastric pH the options are limited to placing a naso-gastric tube (*78*)(invasive and uncomfortable), performing upper endoscopy with gastric aspirate (invasive and expensive) or administering the SmartPill® (*79*). The SmartPill® is a non-biodegradable swallowable electronic device capable of wirelessly transmitting pH information after ingestion. It is expensive and can become retained within the intestine if there are any stenoses or blockages. SmartPill® is made by MEMS (Micro-Electro-Mechanical Systems)-based processes that use materials (e.g., Cu) foreign to the GI tract (*80*). Because of the non-edible materials used in the ingestible electronics, there are safety concerns. A digestible device made of inexpensive components would be safer and potentially less expensive.

Accordingly, real-time measurement of pH values in the GI tract has significant medical importance. Patients with acid secretory disorders (gastroesophageal reflux disease, peptic ulcer disease, Zollinger-Ellison syndrome) would benefit from regular

intermittent monitoring of gastric pH particularly if this could be done inexpensively and safely.

In the present study, a pH sensor was constructed and tested. The present study significantly enables edible electronics with the potential to advance an emerging domain of biomedical technologies and devices.

4.2. Experimental Section

4.2.1. Preparation of shadow mask

The pattern of the mask was designed in AutoCAD and was transferred into a Mylar film (0.1 mm in thickness) using a laser cutter (VLS 6.60 laser cutter, Universal Laser System, Inc.). The laser cutter would cut through the Mylar film to make a shadow mask.

4.2.2. Preparation of substrate for pH sensor version 1

Each substrate consists of powdered sugar, xanthan gum and egg white. Powdered sugar (60 g), xanthan gum (0.5 g) and egg white (12 g) were mixed together in a glass bowl by hand mixer. Keeping mixing them until a sticky paste was achieved and most of the powdered sugar was incorporated. Additional powdered sugar (20 g) and the sticky paste were poured on the work bench. Kneading them until a smooth and non-sticky dough was formed. The sugar paste dough was divided by 8 pieces. Each of them was rolled out and cut into a 7 cm $\times$ 7 cm $\times$ 0.2 cm piece, followed by drying at room temperature for 12 hrs. Before placing shadow mask on substrate, a uniform egg white layer was coated on the surface of substrate. Egg white will make the surface adhesive against a shadow mask after drying it in oven at 70 ℃ for 8 hrs.

4.2.3. Depositing circuit

Gold was deposited for 200 nm thickness using gold sputter. The shadow masks were removed after deposit and the pH sensor version 1 was just made.

4.2.4. Preparation of substrate for pH sensor version 2

Eudragit L100 (1.5 g) was dissolved in absolute ethyl alcohol (50 g) under magnetic stirring (700 rpm) at room temperature and stirred for 15 min until completely dissolved. Glycerol (1.2 g) was added to the solution under magnetic stirring (700 rpm) and stirred for 10 min. Glass Petri dish with 200mm diameter was sprayed by no-stick baking spray. Eudragit L100 solution was poured into the glass petridish and dried at room temperature for 18 hrs. Then the film was peeled off and cut into pieces with dimension of 105 × 22 × 0.3 mm. A shadow mask was placed on the substrate and fixed by tapes.

4.2.5. Preparation of substrate for pH sensor version 3

Gelatin solution was prepared by dissolving gelatin (6 g) in distilled water (50 g) under magnetic stirring (700 rpm) at 70 ℃ and stirred for 15 min. Then glycerol (3 g) was added into the solution under magnetic stirring (700 rpm) and stirred for 10 min. Finally, the solution was poured into bakeware with 20 cm diameter and dried in oven at 80 ℃ for 24 h. The Eudragit L100 coating solution was prepared by dissolving Eudragit (5 g) into absolute ethyl alcohol (10 g). Gelatin film was then coated by 1mm thick Eudragit L100 coating solution using screen coating technology and dried for 5 min. The other side of gelatin film was coated using the same way. Finally, the coating process on

both side of gelatin film was repeated once again. The film was peeled off and cut into pieces with dimension of 100 ×10 ×0.2 mm. A shadow mask was placed on the substrate and fixed by tapes.

4.2.6. Depositing circuit on pH sensor version 2 and 3

The substrates of pH sensor version 2 and 3 were then placed in a vacuum chamber of gold sputtering machine, where gold was deposited on the substrate through the shadow mask, with thickness of 200 nm. Finally, the shadow mask was removed.

4.2.7. Fabrication of pH sensor version 2 and 3

The surface with antenna and capacitor pattern was coated by 1mm thick Eudragit L100 coating solution which was made in the preparation of substrate step using solution using screen coating technology and dried for 5 min. Then a second layer of Eudragit L100 coating was coated in the same way. The gelatin coating solution was prepared by dissolving gelatin (2 g) into distilled water (10 g). The surface of sample with electrodes pattern was coated by 1mm thick gelatin coating solution using screen coating technology and dried for 1 h. The illustrate figure of the coating was shown in Figure 4.1 (a) and (b).

(a)

(b)

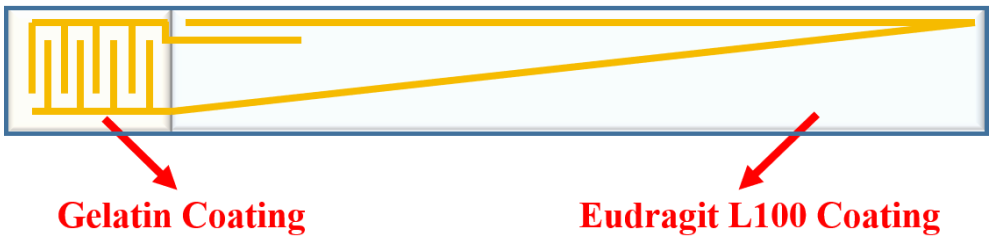

Figure 4.1 Illustration of coating on (a) pH sensor version 2, (b) pH sensor version 3

The remained Eudragit L100 coating solution was put into oven and dried at 80 ℃ for 10 min to form a sticky and glue-like solution. The sample was rolled onto stainless steel stick (1 mm in diameter) which will be draw out later to form a cylinder shape. During rolling, the surface with gold pattern faced outside and the end with antenna was rolled first. Finally, the end of the sample with electrodes was sticked to itself using the glue-like Eudragit L100 solution.

4.2.8. Characterization of devices

The working mechanism (*57*, *58*) is that for acidic solutions, the H^+ residing at the ZnO surface can protonate or deprotonate, $ZnO_{(S)} + H_S^+ \Leftrightarrow Zn(OH)^+$ leading to a surface charge and a surface potential, thus it is pH-sensitive. For basic solutions, with increasing OH^- hydroxyl complexes such as $Zn(OH)_3^-$ will appear,

$ZnO_{(S)} + 2H_2O \Leftrightarrow Zn(OH)_3^- + H_S^-$.

4.3. Result and Discussion

The edible pH sensor version 1 consisting of Au–ZnO as working electrodes, an antenna made of Au for wirelessly transmitting signals, and an edible capacitor, was fabricated on a sugar paste substrate (Figure 4.2 a, b). The reaction of ZnO with either acidic or basic solutions (Acidic: $ZnO_{(S)} + H_S^+ \Leftrightarrow Zn(OH)^+$, basic: $ZnO_{(S)} + 2H_2O \Leftrightarrow Zn(OH)_3^- + H_S^-$) resulted in a change in the capacitance C between Au and ZnO electrodes, and thus the resonant frequency of the pH sensor changed with the pH value via $f = \frac{1}{2\pi\sqrt{LC}}$, where L is the inductance of the antenna that does not depend on the pH value. To validate and calibrate the edible pH sensor, the pH values of reference solutions were measured via a standard pH meter (Hanna Instruments); the capacitance of the Au–ZnO electrodes were characterized utilizing a probe station with precision LCR meter (Hewlett-Packard); and the resonant frequency of the pH sensor was detected by a circuit consisting of a reader, a differential amplifier, a signal generator, and an oscilloscope (Figure 4.3). In the calibration, the edible pH sensors were immersed in the standard solutions with pH values from 1 to 12. As shown in Figure 4.4, the capacitance varied with the pH values. Based on the measured pH-dependent capacitance C, the resonant frequency of the pH sensor was calculated using $= \frac{1}{2\pi\sqrt{LC}}$, where L = 6.1 μH and was separately measured, which is also shown in Figure 4.4. It is apparent that the calculated resonant frequency agreed very well with the measured values. Our results demonstrate that the edible pH sensor was able to measure the pH value of solutions that are both acidic and basic.

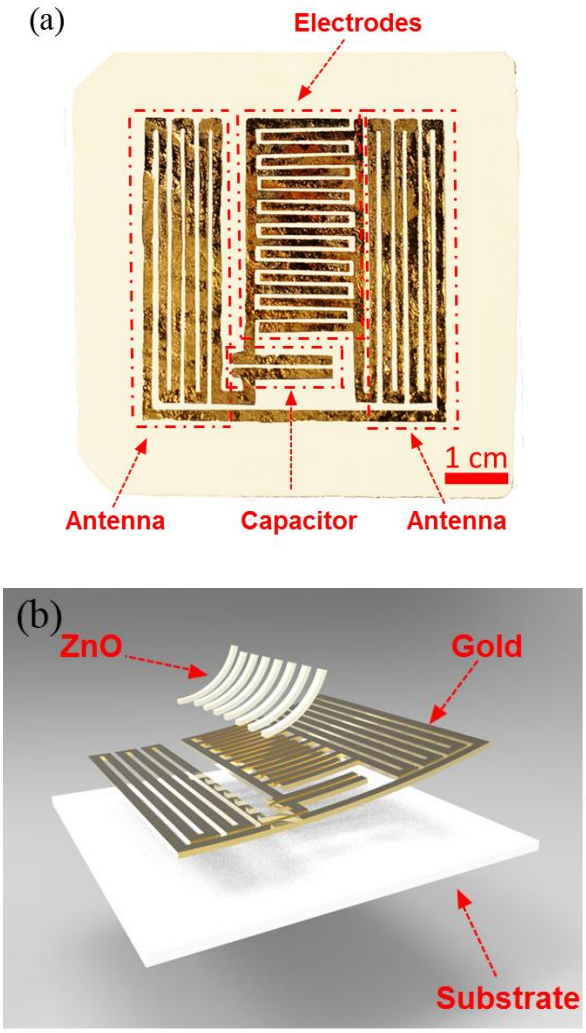

Figure 4.2 (a) Photograph of pH sensor version 1, (b) Illustration of pH sensor version 1

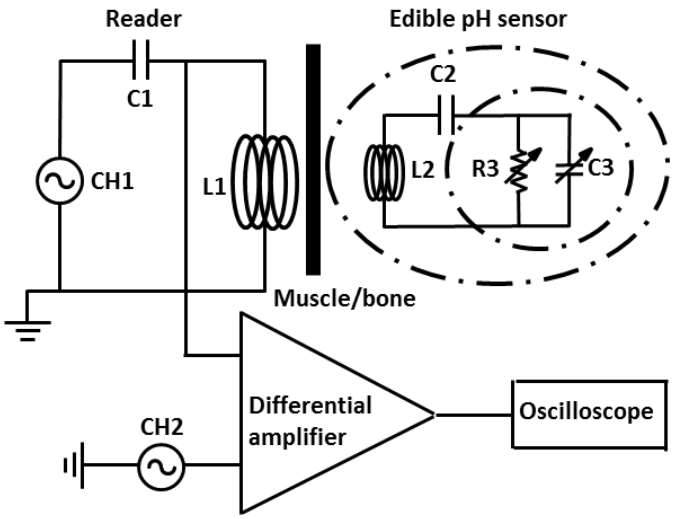

Figure 4.3 Illustration of the working principal and detection scheme of the pH sensor

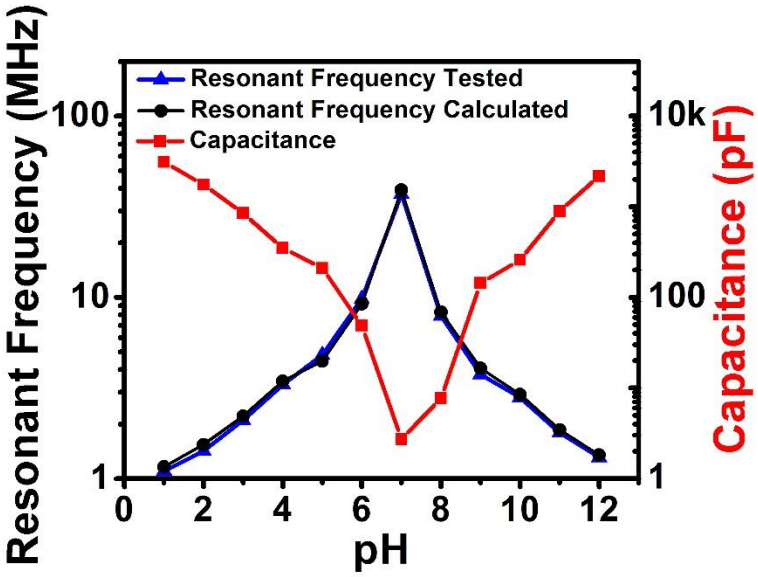

Figure 4.4 Characterization of the edible pH sensor in solutions with pH value from 1 to 12

In the practical application, patient needs to swallow the pH sensor through throat into gastrointestinal tract. In the next study, the overall structure and pattern of conductive circuits are also re-designed delicately to deduce size so that it can be swallowed easily. Gastric residence time is another important factor that determines the

value of the swallowable pH-sensor. Typically, the gastric residence time varies from a few minutes for liquids to a few hours for proteins and fats. Therefore, the ability to control the digestible time of the substrate of the pH sensor was studied. The materials of encapsulation layer and substrate are modified so that the digestive time can be precisely controlled. Also, pH sensor version 2 is portable compared with pH sensor version 1. The substrate of version 1 is sugar paste which is quite brittle when dried. In version 2, more flexible and thinner film was used as the substrate. pH sensor version 2 and 3 have the same diagnosis mechanism with the pH sensor version 1. The following paragraphs will introduce them separately.

The key materials used in this pH sensor is the substrate and coating materials which allow the pH sensor work in the stomach without being damaged and dissolve in the intestine. Researchers developed a Eudragit system which is a family of targeted drug delivery coating polymers. Chemical structure of Eudragit system shows in Figure 4.5.

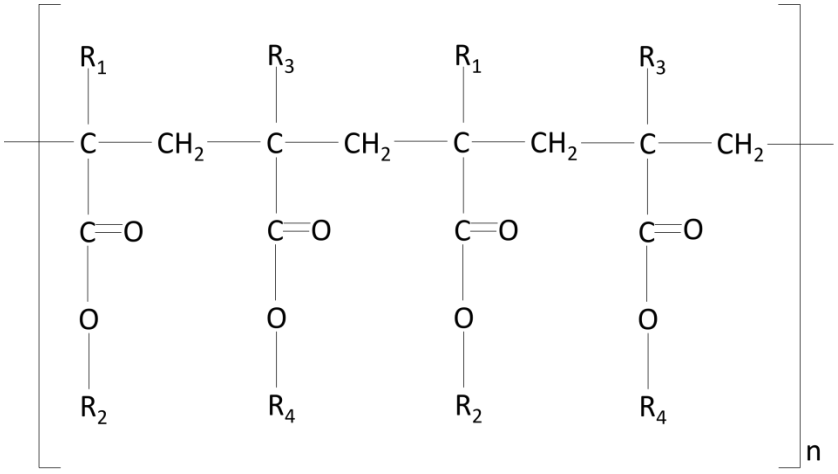

Figure4.5 Chemical structure of Eudragit system. For Eudragit E: R1, R3═CH_3, R2═$CH_2CH_2N(CH_3)_2$, R4═CH_3, C_4H_9 For Eudragit L and Eudragit S: R1, R3═CH_3, R2═H, R4═CH_3 For Eudragit FS: R1═H, R2═H, CH_3, R3═CH_3, R4═CH_3 For Eudragit RL and Eudragit RS: R1═H, CH_3, R2═CH_3, C_2H_3, R3═CH_3, R4═$CH_2CH_2N(CH_3)^+_3Cl^-$ For Eudragit NE 30 D and Eudragit NE 40 D: R1, R3═H, CH_3, R2, R4═CH_3, C2H_3 For Acryl-EZE and Acryl-EZE MP; Eudragit L 30 D-55 and

Eudragit L 100-55, Eastacryl 30 D, Kllicoat MAE 30D, and Kollicoat MAE 30 DP: R1, R3═H, CH_3, R2═H, R4═CH_3, C_2H_3.

Some types are commercially available and comes as the dry powder, aqueous dispersion or organic solution. Depending on the functional groups used in the polymer, Eudragit formulations can be tuned to the type of drug release-immediate, delayed or sustained. Besides drug coating, Eudragit system also have applications in colon targeting, taste masking, radioprotection, intestinal epithelium and corneal permeation and better permeation across skin. (Figure 4.6)

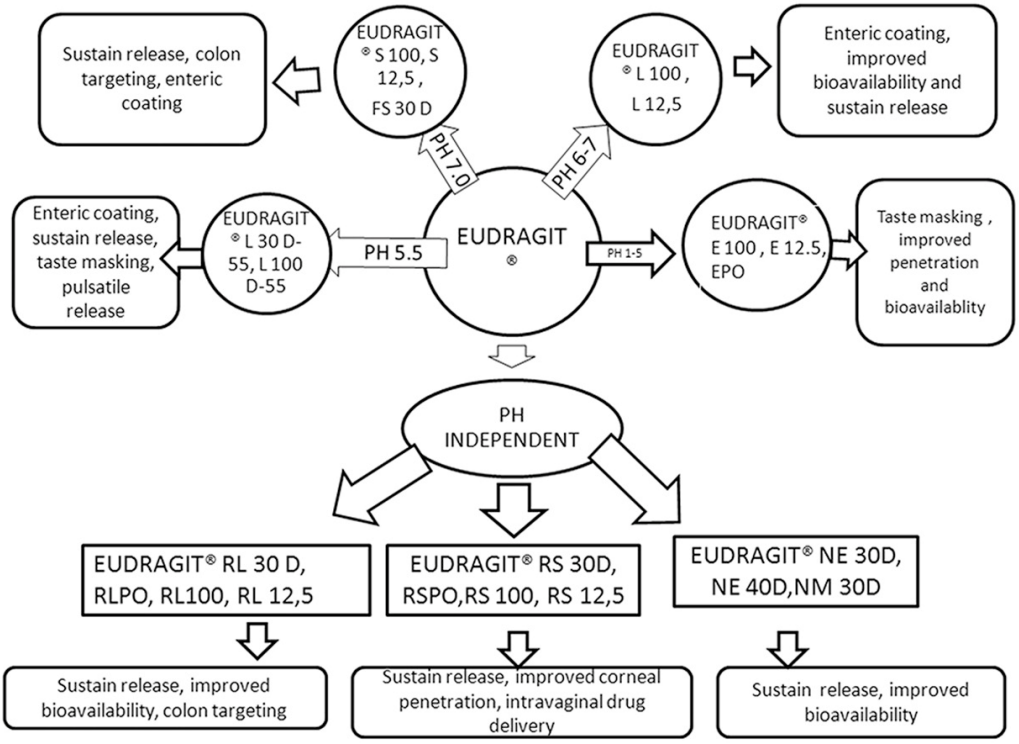

Figure 4.6 Eudragit chemical system and their applications

Before choosing the desire material to use in this project, it is significant to know the pH values in human digestive system. Figure 4.7 shows the pH value in each part of the digestive system along with average time spends. pH sensor was designed to work in the

stomach and dissolve in the intestine. So, the substrate and coating materials should be among the Eudragit L system whose dissolution pH is 5.5.

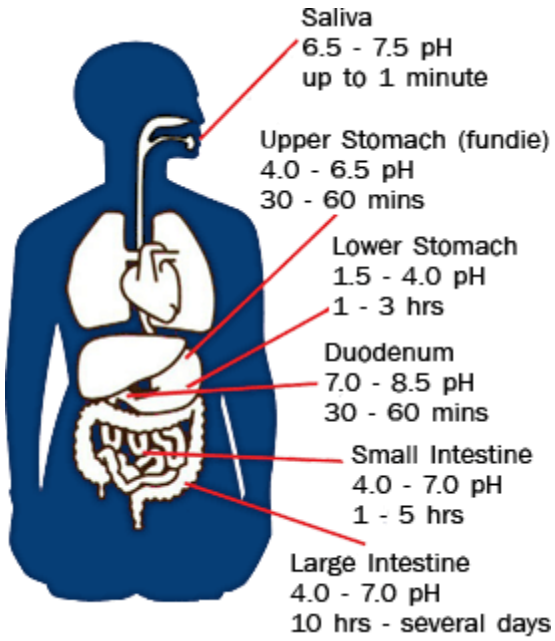

Figure 4.7 pH value in each part of digestive system along with average time spends

In Eudragit L family, Eudragit L100 dissolves at pH above 6. Targeted drug release area of this polymer is jejunum. It has a stable property in stomach and effectively dissolution in intestine. Eudragit L100 is a methacrylic acid and methyl methacrylic acid copolymer with a ratio of 1:1. (Chemical structure shown in Figure 4.8) Its molecular weight is 125000 g/mol, acid value 315 mg KOH/g and glass transition temperature around 110 ℃.

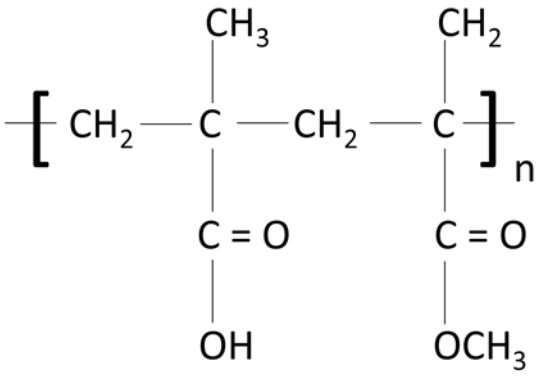

Figure 4.8 Chemical structure of Eudragit L100

So Eudragit L100 was used as the substrate material for pH sensor version 2. Photograph of pH sensor version 2 is shown in Figure 4.9. New design of gold circuit was deposited on the surface of Eudragit L100 substrate by sputtering machine. Figure 4.10 a and b show the structure and dimension of pH sensor version 2. Then the antenna and capacitor circuit parts were coated with Eudragit L100 coating to protect them from stomach fluid. The electrodes part was coated with gelatin coating to protect it from rub and push in the stomach. The gelatin coating swelled and absorbed stomach fluid as soon as it contacted with the stomach fluid. Finally the substrate was rolled into a cylinder with 22mm length and 5mm diameter. (Figure 4.10 b) With this size, pH sensor can be packaged into a commercial size 000 capsule. When the electrodes were contacted and reacted with stomach fluid, the capacitance C between Au and ZnO electrodes would change. Thus the resonant frequency of the pH sensor changed with the pH value according to the equation $f = \frac{1}{2\pi\sqrt{LC}}$, where L is the inductance of the antenna that does not depend on the pH value. The pH - resonant frequency of the pH sensor version 2 is same with the pH sensor version 1's. (Figure 4.5)

Figure 4.9 Photograph of pH sensor version 2

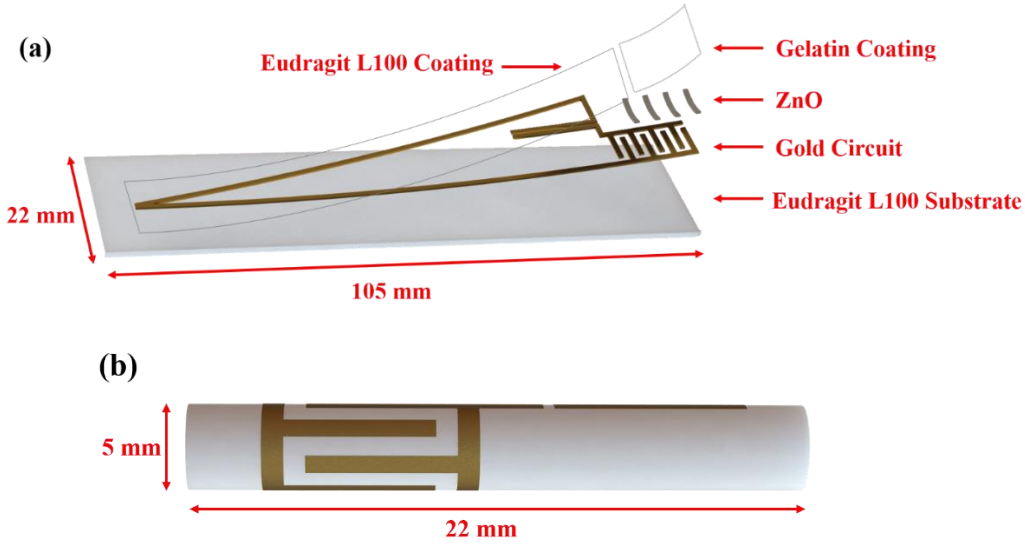

Figure 4.10 Illustration of pH sensor version 2: (a) before rolled (b) after rolled

Pure Eudragit L100 film is brittle. Plasticizer was added to reduce the glass transition temperature and make the Eudragit L100 film more flexible. Plasticizer can reduce the van der Waals forces and hydrogen bonds between the polymer chains and force them apart. Once the polymers are apart, molecular rigidity is relieved, and the polymer film is flexible. Glycerol as a plasticizer has been used before in the previous project. It was also used as plasticizer in this project to make the Eudragit L100 film

more flexible. It had a influence on the dissolution rate of the Eudragit L100 film. So the dissolution time of pH sensor version can be tuned by changing the ratio of Eudragit L100 and glycerol. Figure 4.11 shows that the dissolution time has been prolonged by increasing the amount of Eudragit L100 in solution with pH of 8. It can be attributed to facilitated water penetration, resulting in accelerated polymer ionization and dissolution. (*81, 82*) When the content of Eudragit L100 was higher than 50%, the film became brittle which made it difficult to be rolled. While if the content of Eudragit L100 was lower than 50%, excess glycerol will spread over the surface of film. So in the following study, a content of 50% was used. The dissolution time of pH sensor version 2 made with film in whcih Eudragit L100's content is 50% has been investigated in solutions with different pH value. In Figure 4.12 it is clear that pH sensor version 2 doesn't dissolve in acid solution. The dissolution time decreased as the pH value increased. Figure 4.13 shows the process of pH sensor version 2's dissolution in solution with pH 8.

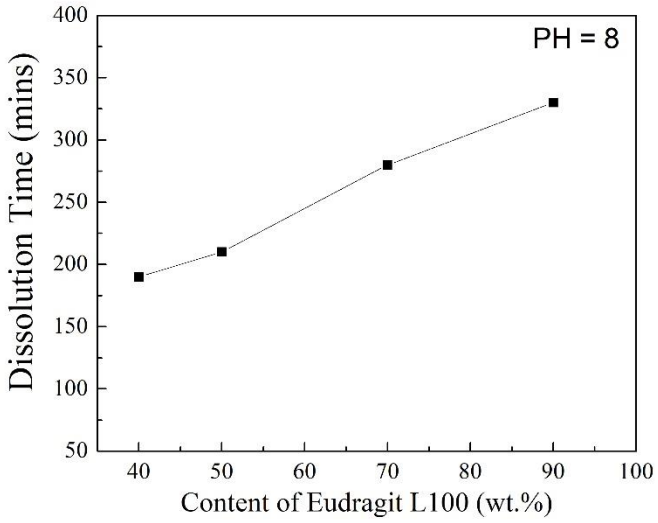

Figure 4.11 Dissolution time of pH sensor version 2 with different content of Eudragit L100

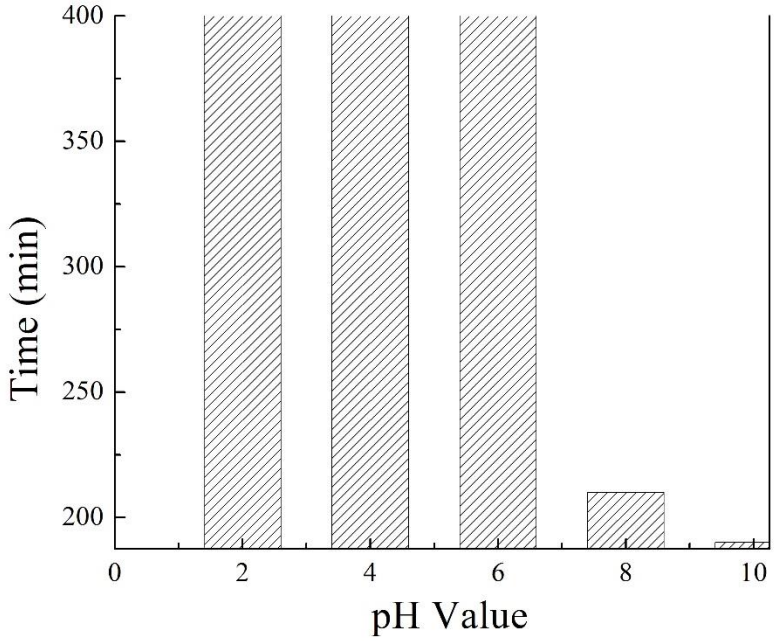

Figure 4.12 Dissolution time of pH sensor version 2 in solutions with different pH value

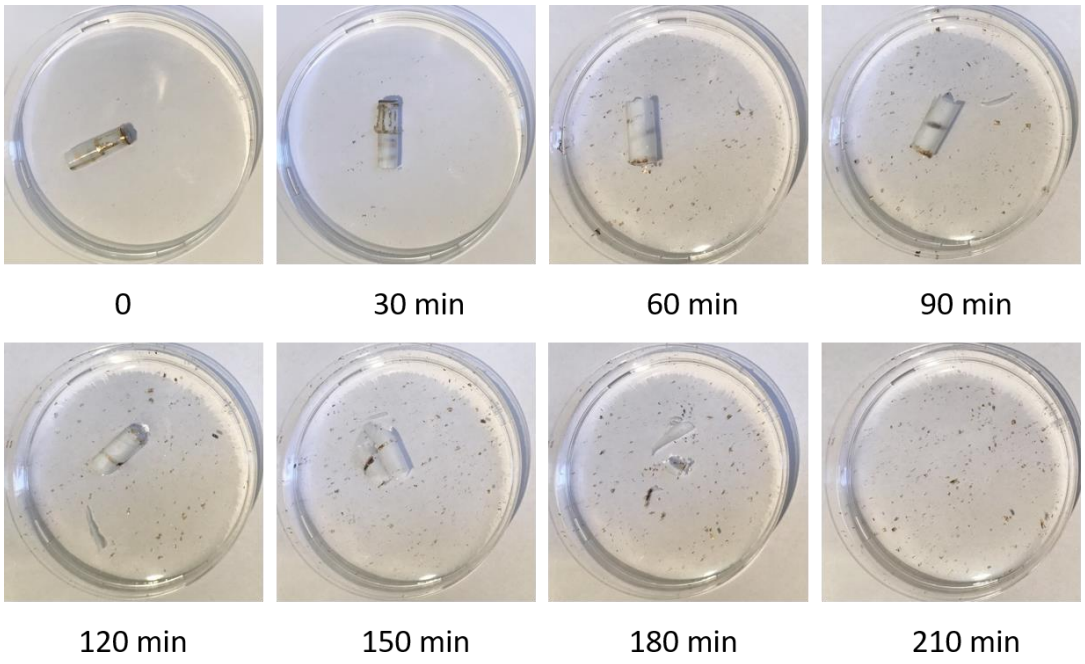

Figure 4.13 The dissolution process of pH sensor version 2 in pH 8 solution

After pH sensor version 2, a pH sensor version 3 which had a smaller size and shorter digestive time was designed. The substrate of this new version pH sensor had a sandwich structure which was Eudragit L100 – Gelatin – Eudragit L100. Gelatin film was more flexible and thinner than Eudragit L100 film. It can be made as thin as 100 μm. The circuit was also redesigned after calculation to make the sensor smaller. Figure 4.14 and 4.15 a, b show the photo and illustration of pH sensor version 3. The dissolution time of pH sensor version 3 in pH 8 solution was 3 hr. Figure 4.16 shows the test process. Prof. Jiang swallowed the pH sensor version 3 with 150ml water. The red pan in Figure 4.16 b and d is a signal reader which should be place in front of human body with a distance within 20 cm. The signal reader was coupled with a controller that can transmit data wirelessly to a cell phone for easy data communication, processing and display. pH value can be read on the phone within 6 sec after the sensor was swallowed. The pH value of

Prof. Jiang's empty stomach was 1.8. Then the pH value was tested again after 10 min, the result was still 1.8. Finally Prof. Jiang drank 150ml water, the pH value turned to 2.0. This set of photos demonstrates that edible pH sensor can test the pH value fast, accurate and stable.

Figure 4.14 Photograph of pH sensor version 3

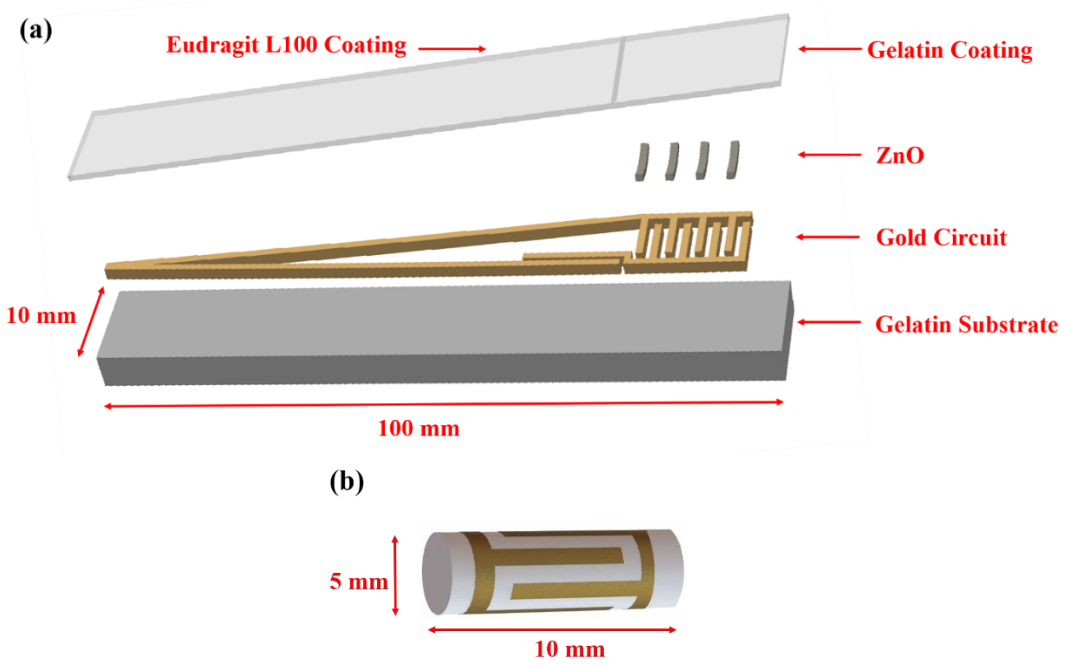

Figure 4.15 Illustration of pH sensor version 3

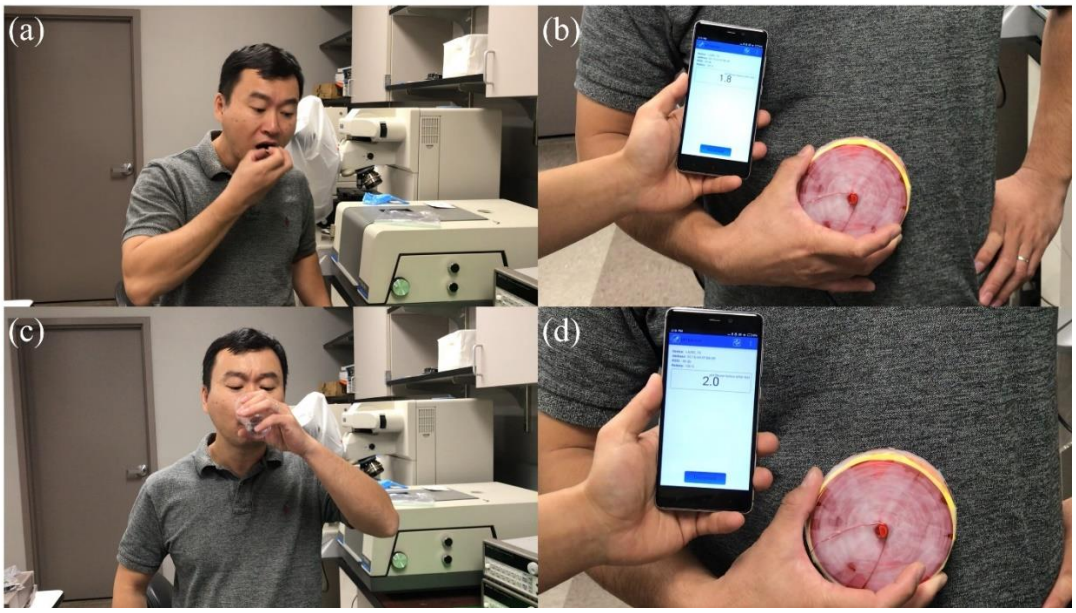

Figure 4.16 Photograph of the test process

CHAPTER 5 EDIBLE GEL ELECTROLYTE

5.1. Background and motivation

A supercapacitor needs not only good electrochemical performance but also reliable safety performance. Majority supercapacitors are using liquid electrolytes. If the liquid electrolyte could be replace with solid electrolyte, the safety of supercapacitors would be largely enhanced by reducing the electrolyte leakage and corrosion. Gel polymer electrolyte is a promising candidate for enhancing device safety and providing higher ionic conductivity than the polymeric solid electrolytes. And the target of this side project is to develop an edible gel electrolyte with good mechanical properties for edible supercapacitor. Back to the first project in this prospectus, variety kinds of electrolyte were used to build an edible supercapacitor. One of the electrolytes was Jello. Just like the common hydrogel, Jell also suffer from a lack of mechanical toughness. This brittle electrolyte will induce the short circuit of edible supercapacitor because the two electrodes contact with each other. So an edible gel which could have good ionic conductivity as well as appropriate mechanical properties is significant.

A novel method for developing hydrogels with high mechanical toughness was reported by Gong's group. (*83*) The hydrogels consisted of two kinds of hydrophilic polymer, one has relative long chain and the other on has a relative short chain, forming a double-network (DN) structure. A cross-linker was used to enhance the double network.

All the materials that were chosen should be edible. Gelatin as a common component for hydrogel was chosen to work as the relative short chain structural polymer because it is edible. Gluten is a water insoluble protein that is formed when water is

mixed with wheat flour. It served as the relative long chain polymer. Genipin served as the cross-linker. It is a natural chemical compound in gardenia fruit extract. It is also an excellent natural cross-linker for proteins, collagen, gelatin and chitosan cross linking. Genipin could cross link polymer by reacting with the primary amino group in other polymers. There are two reaction schemes (shown in Figure 5.1) for crosslinking reactions involving genipin. (*84*) The double network structure of tough hydrogel consists of gelain and gluten crosslinked with genipin was shown in Figure 5.2.

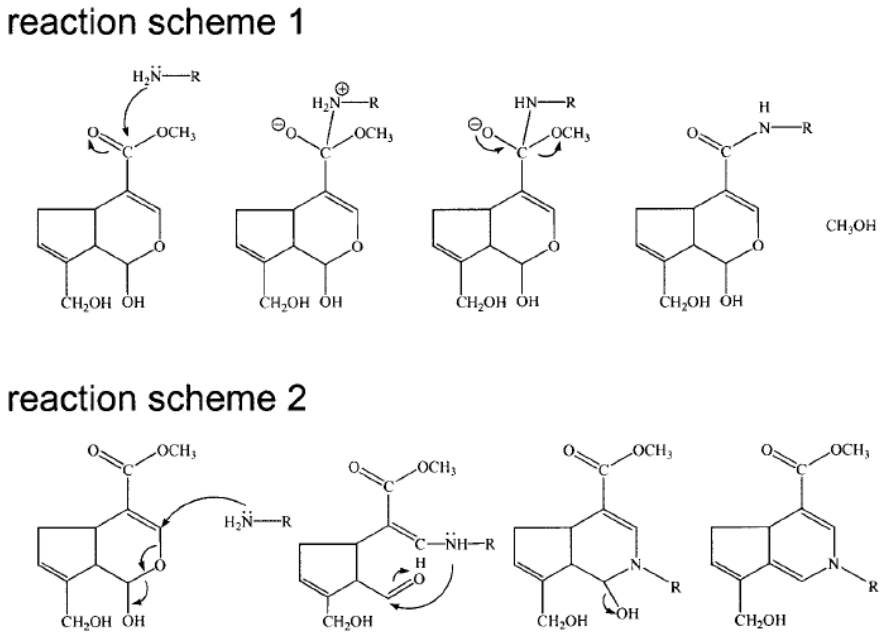

Figure 5.1 Crosslinking reactions involving genipin

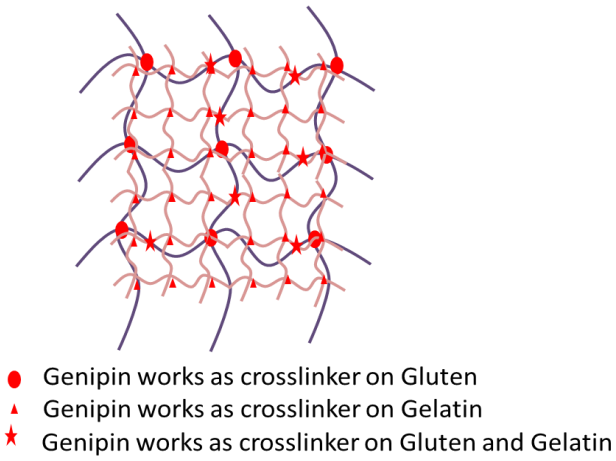

Figure 5.2 Schematic of structure of genipin crosslinked gluten and gelatin

5.2. Experimental Section

5.2.1. Preparation of gluten

140 g bread flour and 90 ml 40 ℃ deionized water (DI water) were mixed in a glass container. The mixture was kneaded for 20 min until a dough with smooth surface was formed. Dough was placed in a 40 ℃ oven for 40 min for self-fermentation. Then the raw gluten was obtained by washing the dough completely with water until the water was clear. 0.5 g yeast was dissolved in 20 ml 40 ℃ DI water. Raw gluten and yeast solution were kneaded for 5 min followed by fermenting in an oven for 4 h at 50 ℃. The fermented raw gluten was steamed in a steamer under high heat for 20 min.

5.2.2. Preparation of tough hydrogel

Gluten made in 5.2.1 was cut in to four 2*2*2 cm cubes. Gelatin sheet with 2 g was immersed in to 40 ml DI water in a beaker for 30 min to be fully bloomed. Then the mixture was heated to 100 ℃ to dissolve gelatin under magnetic stir for 20 min. The temperature of the heater was adjusted to 50 ℃. Gluten cubes was put into the gelatin

solution and pressed to absorb solution completely. Then magnetic stirred the gluten in gelatin solution for 20 min. 0.01 g genipin was added into the baker and stirred for 4 h. Finally, the beaker was placed under room temperature overnight (10 h).

5.3. Result and Discussion

Gluten consists of gliadin and glutenin which are two main proteins in wheat flour. The structure of gluadin and glutenin are shown in Figure 5.3. Gladins are mainly monomeric proteins with molecular weights (MWs) around 28,000-55,000. Glutenin has a varying size ranging from 500,000 to more than 10 million. When sufficient water is added to dry wheat flour the two proteins become flexible and able to move about. The process of wetting the proteins is called hydration. As water and flour are mixed the hydrated proteins are brought together and begin to interact. They begin to stick to each other through the formation of chemical bonds. These bonds are called disulfide bonds. (Figure 5.4) Also the process of kneading could help the hydrated flexible proteins become stretched and aligned in the direction of kneading which provides more opportunities to form cross links between the proteins. Stretchy and sticky gluten will be filled with thousands of CO_2 gas bubbles as the yeast goes to work under 50 ℃. During the steaming, the CO_2 gas bubbles will swell and come out. Gluten will become porous with large pores with 1-2 mm and micro pores with 10-20 μm. (shown in Figure 5.5)

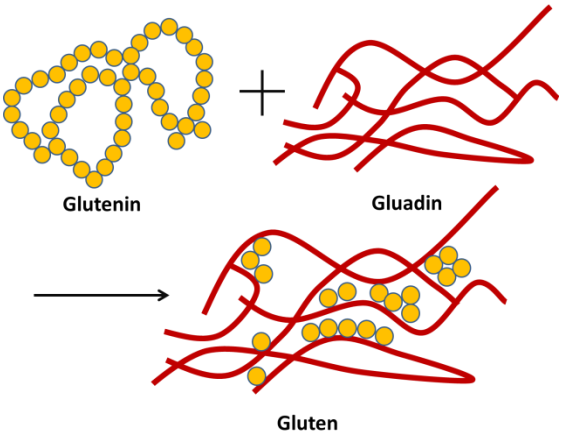

Figure 5.3 Schematic of the relationship among glutenin, gluadin and gluten.

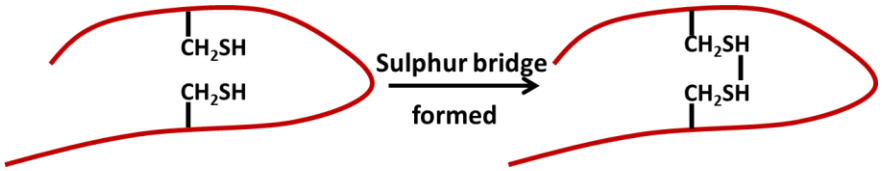

Figure 5.4 The disulfide bonds between chains of proteins.

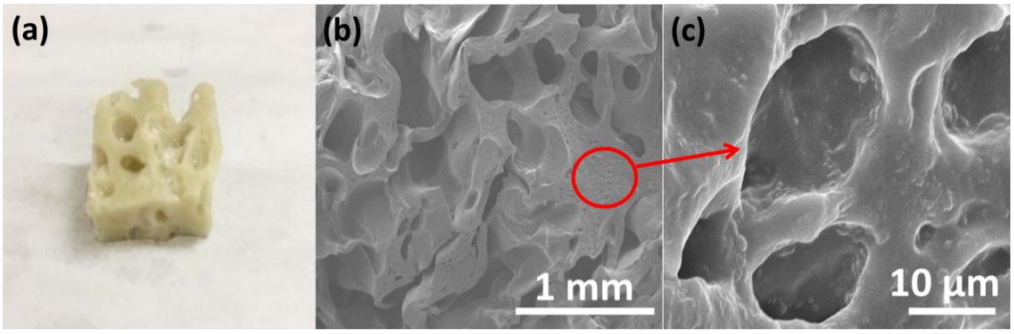

Figure 5.5 (a) Photograph of gluten (b) and (c) SEM figures of gluten

The photographs of gelatin, genipin crosslinked gelatin, gluten and genipin crosslinked gluten and gelatin are shown in Figure 5.6. The crosslinked products are blue because a dark blue pigment will be obtained from the reaction of genipin with primary

amines in the proteins. This blue pigment has been used in the fabrication of heat, pH and light resistant food dyes.

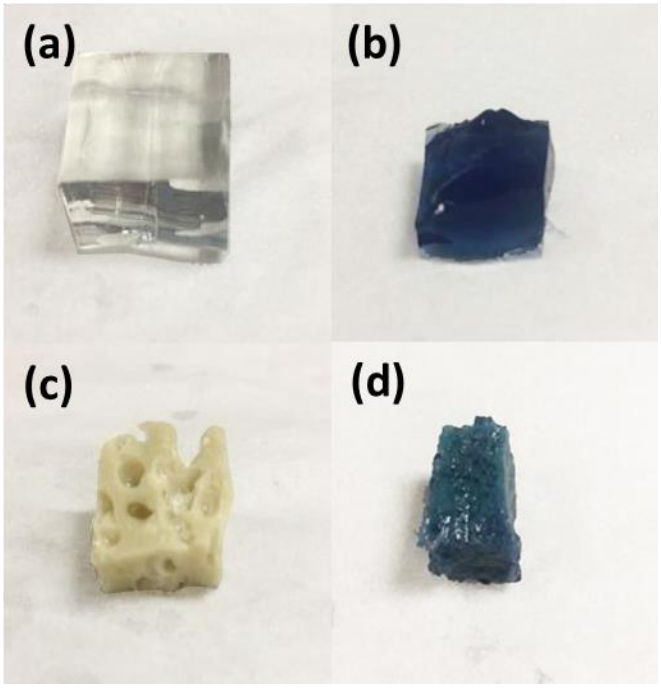

Figure 5.6 Photographs of (a) gelatin gel (b) genipin corsslinked gelatin gel (c) gluten (d) genipin crosslinked gluten and gelatin

CHAPTER 6 Summary and Future Work

6.1. Summary

In summary, history, advantage and composition are studied in the first chapter of this dissertation. Fabrication process of making different edible components and devices are then demonstrated in followed chapters.

The edible supercapacitor presented the chapter 2 is the first one that is truly edible and digestible as all components are explicitly originated from food (not food grade), which is different from other endeavors on edible electronics or edible energy storage devices. The edible supercapacitors have demonstrated their ability to serve as an electrical “antibacterial” for killing bacteria in vitro and to power a commercial USB camera. In addition to its antibacterial properties, may be used as an oncological adjuvant for alimentary and other malignancies.

Besides natural food materials, processed food materials were introduced in chapter 3. Materials derived from natural foods serve as dominant elements in the fabrication of electronic components and devices and that any gaps in properties not provided by these materials, may be filled in with edible processed foods, food components and on a limited basis non-toxic levels of electronic materials to create full constructs. A “preferred food kit” was created for component fabrication using natural and processed food materials. Specific individual and combined components were built and characterized utilizing the preferred food kit. By merging modern food engineering, materials science, device fabrications, and biomedical applications, this work has the potential to broadly and

deeply impact the field of edible electronics as the horizon of search candidate materials for edible electronics has been unprecedentedly expanded.

In Chapter 4, a pH sensor made by edible materials is constructed and tested. Edible pH sensor can be swallowed and measure pH values in the GI tract real-time. Edible pH sensor is low-cost since all the components are inexpensive. Finally, this pH sensor can be digested in the intestine and passed out human body.

In Chapter 5, genipin crosslinked gluten and gelatin which has good ionic conductivity as well as appropriate mechanical properties is demonstrated. This crosslinked gel has a potential to work as a solid electrolyte for edible supercapacitor.

6.2. Future Work

Common capsule materials are not deformable. They usually either dissolve in the stomach fluid or not. Their dissolution time in the stomach can't be controlled. To enrich the capsule materials for edible pH sensor, a capsule which is flexible, stretchable and controllable need to be studied.

The ideal package materials should have the following properties:

1 Flexible and stretchable.

2 Tough. The package materials should have the enough toughness to protect filling materials from the movement of stomach.

3 Partially acid resistant. Materials should degrade slowly in the stomach fluid. The degradation time can be controlled.

Hydrogel is a good choice to work as the package material. They have various applications such as microfluidics, contact lenses, drug delivery system, and gel electrolyte. Although most of the hydrogel suffer from a lack of mechanical strength, double network hydrogel possess a tough and stretchable properties. In the future, some biocompatible and biodegradable materials will be considered to make a crosslinked double network hydrogel such as alginate, PLGA, PLA, PEG and so on. Gum may be added to the hydrogel to improve the stretchability.

REFERENCES

1. G. Deuschl, C. Schade-Brittinger, P. Krack, J. Volkmann, H. Schäfer, K. Bötzel, C. Daniels, A. Deutschländer, U. Dillmann, W. Eisner, A randomized trial of deep-brain stimulation for Parkinson's disease. *New England Journal of Medicine* **355**, 896-908 (2006).

2. E. Ben-Menachem, R. Mañon-Espaillat, R. Ristanovic, B. Wilder, H. Stefan, W. Mirza, W. Tarver, J. Wernicke, Vagus nerve stimulation for treatment of partial seizures: 1. A controlled study of effect on seizures. *Epilepsia* **35**, 616-626 (1994).

3. A. Assaf, S. Hillerup, J. Rostgaard, M. Puche, M. Blessmann, C. Kohlmeier, P. Pohlenz, J. Klatt, M. Heiland, A. Caparso, Technical and surgical aspects of the sphenopalatine ganglion (SPG) microstimulator insertion procedure. *International journal of oral and maxillofacial surgery* **45**, 245-254 (2016).

4. J. Pickup, H. Keen, Continuous subcutaneous insulin infusion at 25 years. *Diabetes care* **25**, 593-598 (2002).

5. W. V. Tamborlane, R. S. Sherwin, M. Genel, P. Felig, Reduction to normal of plasma glucose in juvenile diabetes by subcutaneous administration of insulin with a portable infusion pump. *New England Journal of Medicine* **300**, 573-578 (1979).

6. V. Parsonnet, S. Furman, N. P. SMYTH, Implantable cardiac pacemakers status report and resource guideline: Pacemaker Study Group. *Circulation* **50**, page5-A-35 (1974).

7. W. A. Qureshi, Current and future applications of the capsule camera. *Nature reviews drug discovery* **3**, 447-450 (2004).

8. G. Iddan, G. Meron, A. Glukhovsky, P. Swain, Wireless capsule endoscopy. *Nature* **405**, 417 (2000).

9. G. Costamagna, S. K. Shah, M. E. Riccioni, F. Foschia, M. Mutignani, V. Perri, A. Vecchioli, M. G. Brizi, A. Picciocchi, P. Marano, A prospective trial comparing small bowel radiographs and video capsule endoscopy for suspected small bowel disease. *Gastroenterology* **123**, 999-1005 (2002).

10. M. Koziolek, M. Grimm, D. Becker, V. Iordanov, H. Zou, J. Shimizu, C. Wanke, G. Garbacz, W. Weitschies, Investigation of pH and temperature profiles in the GI tract of fasted human subjects using the Intellicap® system. *Journal of pharmaceutical sciences* **104**, 2855-2863 (2015).

11. M. N. Antipina, G. B. Sukhorukov, Remote control over guidance and release properties of composite polyelectrolyte based capsules. *Adv Drug Deliv Rev* **63**, 716-729 (2011); published online EpubAug 14 (10.1016/j.addr.2011.03.012).

12. J. S. Kroin, R. J. McCarthy, L. Stylos, K. Miesel, A. D. Ivankovich, R. D. Penn, Long-term testing of an intracranial pressure monitoring device. *Journal of neurosurgery* **93**, 852-858 (2000).

13. S.-W. Hwang, H. Tao, D.-H. Kim, H. Cheng, J.-K. Song, E. Rill, M. A. Brenckle, B. Panilaitis, S. M. Won, Y.-S. Kim, A physically transient form of silicon electronics. *Science* **337**, 1640-1644 (2012).

14. X. Huang, Y. Liu, S. W. Hwang, S. K. Kang, D. Patnaik, J. F. Cortes, J. A. Rogers, Biodegradable materials for multilayer transient printed circuit boards. *Advanced Materials* **26**, 7371-7377 (2014).

15. S.-W. Hwang, C. H. Lee, H. Cheng, J.-W. Jeong, S.-K. Kang, J.-H. Kim, J. Shin, J. Yang, Z. Liu, G. A. Ameer, Biodegradable elastomers and silicon nanomembranes/nanoribbons for stretchable, transient electronics, and biosensors. *Nano letters* **15**, 2801-2808 (2015).

16. S. W. Hwang, J. K. Song, X. Huang, H. Cheng, S. K. Kang, B. H. Kim, J. H. Kim, S. Yu, Y. Huang, J. A. Rogers, High-Performance Biodegradable/Transient Electronics on Biodegradable Polymers. *Advanced Materials* **26**, 3905-3911 (2014).

17. S. K. Kang, S. W. Hwang, S. Yu, J. H. Seo, E. A. Corbin, J. Shin, D. S. Wie, R. Bashir, Z. Ma, J. A. Rogers, Biodegradable Thin Metal Foils and Spin-On Glass Materials for Transient Electronics. *Advanced Functional Materials* **25**, 1789-1797 (2015).

18. L. Yin, X. Huang, H. Xu, Y. Zhang, J. Lam, J. Cheng, J. A. Rogers, Materials, designs, and operational characteristics for fully biodegradable primary batteries. *Advanced Materials* **26**, 3879-3884 (2014).

19. M. Irimia-Vladu, P. A. Troshin, M. Reisinger, L. Shmygleva, Y. Kanbur, G. Schwabegger, M. Bodea, R. Schwödiauer, A. Mumyatov, J. W. Fergus, Biocompatible and Biodegradable Materials for Organic Field-Effect Transistors. *Advanced Functional Materials* **20**, 4069-4076 (2010).

20. M. Irimia-Vladu, E. D. Głowacki, P. A. Troshin, G. Schwabegger, L. Leonat, D. K. Susarova, O. Krystal, M. Ullah, Y. Kanbur, M. A. Bodea, Indigo-A Natural Pigment for High Performance Ambipolar Organic Field Effect Transistors and Circuits. *Advanced Materials* **24**, 375-380 (2012).

21. M. Irimia-Vladu, E. D. Głowacki, G. Voss, S. Bauer, N. S. Sariciftci, Green and biodegradable electronics. *Materials Today* **15**, 340-346 (2012).

22. M. Hussain, J. Xie, Z. Hou, K. Shezad, J. Xu, K. Wang, Y. Gao, L. Shen, J. Zhu, Regulation of drug release by tuning surface textures of biodegradable polymer microparticles. *ACS applied materials & interfaces* **9**, 14391-14400 (2017).

23. S. Doppalapudi, A. Jain, A. J. Domb, W. Khan, Biodegradable polymers for targeted delivery of anti-cancer drugs. *Expert opinion on drug delivery* **13**, 891-909 (2016).

24. R. F. Kempczinski, J. E. Rosenman, W. H. Pearce, L. R. Roedersheimer, Y. Berlatzky, G. Ramalanjaona, Endothelial cell seeding of a new PTFE vascular prosthesis. *Journal of vascular surgery* **2**, 424-429 (1985).

25. R. Thomson, M. Wake, M. Yaszemski, A. Mikos, in *Biopolymers Ii*. (Springer, 1995), pp. 245-274.

26. Y. Khan, M. J. Yaszemski, A. G. Mikos, C. T. Laurencin, Tissue engineering of bone: material and matrix considerations. *JBJS* **90**, 36-42 (2008).

27. D. Linden, in *Fuel and Energy Abstracts*. (1995), vol. 4, pp. 265.

28. H. H. Uhlig, *Uhlig's corrosion handbook*. (John Wiley & Sons, 2011), vol. 51.

29. R. Foresti, M. Hoque, D. Monti, C. J. Green, R. Motterlini, Differential activation of heme oxygenase-1 by chalcones and rosolic acid in endothelial cells. *Journal of Pharmacology and Experimental Therapeutics* **312**, 686-693 (2005).

30. Y. J. Kim, S.-E. Chun, J. Whitacre, C. J. Bettinger, Self-deployable current sources fabricated from edible materials. *Journal of Materials Chemistry B* **1**, 3781-3788 (2013).

31. Y. J. Kim, W. Wu, S.-E. Chun, J. F. Whitacre, C. J. Bettinger, Biologically derived melanin electrodes in aqueous sodium-ion energy storage devices. *Proceedings of the National Academy of Sciences* **110**, 20912-20917 (2013).

32. Z. Li, D. Young, K. Xiang, W. C. Carter, Y. M. Chiang, Towards High Power High Energy Aqueous Sodium-Ion Batteries: The NaTi2 (PO4) 3/Na0. 44MnO2 System. *Advanced Energy Materials* **3**, 290-294 (2013).

33. W. Wu, A. Mohamed, J. Whitacre, Microwave synthesized NaTi2 (PO4) 3 as an aqueous sodium-ion negative electrode. *Journal of The Electrochemical Society* **160**, A497-A504 (2013).

34. H. Yu, J. Wu, L. Fan, K. Xu, X. Zhong, Y. Lin, J. Lin, Improvement of the performance for quasi-solid-state supercapacitor by using PVA–KOH–KI polymer gel electrolyte. *Electrochimica Acta* **56**, 6881-6886 (2011).

35. J. Yan, Q. Wang, T. Wei, Z. Fan, Recent advances in design and fabrication of electrochemical supercapacitors with high energy densities. *Advanced Energy Materials* **4**, (2014).

36. A. Gennadios, A. Handa, G. W. Froning, C. L. Weller, M. A. Hanna, Physical properties of egg white− dialdehyde starch films. *Journal of Agricultural and Food Chemistry* **46**, 1297-1302 (1998).

37. G. Lu, T. Chen, Application of egg white and plasma powders as muscle food binding agents. *Journal of Food Engineering* **42**, 147-151 (1999).

38. D. Siegel, K. Church, G. Schmidt, Gel structure of nonmeat proteins as related to their ability to bind meat pieces. *Journal of Food Science* **44**, 1276-1279 (1979).

39. L. L. Zhang, X. Zhao, Carbon-based materials as supercapacitor electrodes. *Chemical Society Reviews* **38**, 2520-2531 (2009).

40. S. Barranco, J. Spadaro, T. Berger, R. Becker, In vitro effect of weak direct current on Staphylococcus aureus. *Clinical orthopaedics and related research* **100**, 250-255 (1974).

41. C. Davis, N. Wagle, M. Anderson, M. Warren, Bacterial and fungal killing by iontophoresis with long-lived electrodes. *Antimicrobial agents and chemotherapy* **35**, 2131-2134 (1991).

42. T. Matsunaga, S. Nakasono, S. Masuda, Electrochemical sterilization of bacteria adsorbed on granular activated carbon. *FEMS microbiology letters* **93**, 255-259 (1992).

43. T. Matsunaga, S. Nakasono, T. Takamuku, J. G. Burgess, N. Nakamura, K. Sode, Disinfection of drinking water by using a novel electrochemical reactor employing carbon-cloth electrodes. *Applied and environmental microbiology* **58**, 686-689 (1992).

44. Ż. Król, A. Jarmoluk, The effects of using a direct electric current on the chemical properties of gelatine gels and bacterial growth. *Journal of Food Engineering* **170**, 1-7 (2016).

45. J. L. Del Pozo, M. S. Rouse, J. N. Mandrekar, J. M. Steckelberg, R. Patel, The electricidal effect: reduction of Staphylococcus and Pseudomonas biofilms by prolonged exposure to low-intensity electrical current. *Antimicrobial agents and chemotherapy* **53**, 41-45 (2009).

46. E. L. Sandvik, B. R. McLeod, A. E. Parker, P. S. Stewart, Direct electric current treatment under physiologic saline conditions kills Staphylococcus epidermidis biofilms via electrolytic generation of hypochlorous acid. *PloS one* **8**, e55118 (2013).

47. D. A. Nathan, S. Center, C.-y. Wu, W. Keller, An implantable synchronous pacemaker for the long term correction of complete heart block. *The American journal of cardiology* **11**, 362-367 (1963).

48. P. Li, V. Kothari, B. S. Terry, Design and Preliminary Experimental Investigation of a Capsule for Measuring the Small Intestine Contraction Pressure. *IEEE Transactions on Biomedical Engineering* **62**, 2702-2708 (2015).

49. R. Goffredo, A. Pecora, L. Maiolo, A. Ferrone, E. Guglielmelli, D. Accoto, A Swallowable Smart Pill for Local Drug Delivery. *Journal of Microelectromechanical Systems* **25**, 362-370 (2016).

50. F. Munoz, G. Alici, W. Li, A review of drug delivery systems for capsule endoscopy. *Advanced drug delivery reviews* **71**, 77-85 (2014).

51. C. J. Ferris, Conducting bio-materials based on gellan gum hydrogels. *Soft Matter* **5**, 3430-3437 (2009).

52. N. Gontard, S. Marchesseau, J. L. CUQ, S. Guilbert, Water vapour permeability of edible bilayer films of wheat gluten and lipids. *International journal of food science & technology* **30**, 49-56 (1995).

53. S. T. Parker, P. Domachuk, J. Amsden, J. Bressner, J. A. Lewis, D. L. Kaplan, F. G. Omenetto, Biocompatible silk printed optical waveguides. *Advanced Materials* **21**, 2411-2415 (2009).

54. Y. J. Kim, W. Wu, S. E. Chun, J. F. Whitacre, C. J. Bettinger, Catechol-Mediated Reversible Binding of Multivalent Cations in Eumelanin Half-Cells. *Advanced Materials* **26**, 6572-6579 (2014).

55. X. Wang, W. Xu, P. Chatterjee, C. Lv, J. Popovich, Z. Song, L. Dai, M. Y. S. Kalani, S. E. Haydel, H. Jiang, Food-Materials-Based Edible Supercapacitors. *Advanced Materials Technologies* **1**, (2016).

56. J. A. Cracknell, K. A. Vincent, F. A. Armstrong, Enzymes as working or inspirational electrocatalysts for fuel cells and electrolysis. *Chemical Reviews* **108**, 2439-2461 (2008).

57. S. M. Al-Hilli, M. Willander, A. Öst, P. Strålfors, ZnO nanorods as an intracellular sensor for p H measurements. *Journal of Applied Physics* **102**, 084304 (2007).

58. A. Fulati, S. M. Usman Ali, M. Riaz, G. Amin, O. Nur, M. Willander, Miniaturized pH sensors based on zinc oxide nanotubes/nanorods. *Sensors* **9**, 8911-8923 (2009).

59. R. A. Higgins, *Materials for engineers and technicians*. (Routledge, 2010).

60. S. E. Derenzo, *Practical interfacing in the laboratory: using a PC for instrumentation, data analysis and control*. (Cambridge University Press, 2003).

61. E. Fukada, I. Yasuda, On the piezoelectric effect of bone. *Journal of the physical society of Japan* **12**, 1158-1162 (1957).

62. C. Halperin, S. Mutchnik, A. Agronin, M. Molotskii, P. Urenski, M. Salai, G. Rosenman, Piezoelectric effect in human bones studied in nanometer scale. *Nano Letters* **4**, 1253-1256 (2004).

63. A. A. Marino, R. O. Becker, Piezoelectricity in hydrated frozen bone and tendon. *Nature* **253**, 42 (1975).

64. J. Kim, S. Yun, Z. Ounaies, Discovery of cellulose as a smart material. *Macromolecules* **39**, 4202-4206 (2006).

65. J. Y. Fu, P. Y. Liu, J. Cheng, A. S. Bhalla, R. Guo, Optical measurement of the converse piezoelectric d33 coefficients of bulk and microtubular zinc oxide crystals. *Applied physics letters*, (2007).

66. R. Agrawal, H. D. Espinosa, Giant piezoelectric size effects in zinc oxide and gallium nitride nanowires. A first principles investigation. *Nano letters* **11**, 786-790 (2011).

67. T. Kahlon, M. Chapman, G. Smith, In vitro binding of bile acids by spinach, kale, brussels sprouts, broccoli, mustard greens, green bell pepper, cabbage and collards. *Food chemistry* **100**, 1531-1536 (2007).

68. C. Agostoni, E. Riva, M. Giovannini, Dietary fiber in weaning foods of young children. *Pediatrics* **96**, 1002-1005 (1995).

69. J. Yoo, L. Yan, S. Lee, Y. Kim, H. Kim, B. Kim, H.-J. Yoo, in *Solid-State Circuits Conference-Digest of Technical Papers, 2009. ISSCC 2009. IEEE International*. (IEEE, 2009), pp. 290-291,291 a.

70. L. Yan, J. Bae, S. Lee, T. Roh, K. Song, H.-J. Yoo, A 3.9 mW 25-electrode reconfigured sensor for wearable cardiac monitoring system. *IEEE Journal of Solid-State Circuits* **46**, 353-364 (2011).

71. J. Yang, D. Wei, L. Tang, X. Song, W. Luo, J. Chu, T. Gao, H. Shi, C. Du, Wearable temperature sensor based on graphene nanowalls. *Rsc Advances* **5**, 25609-25615 (2015).

72. T. Q. Trung, S. Ramasundaram, B. U. Hwang, N. E. Lee, An all-elastomeric transparent and stretchable temperature sensor for body-attachable wearable electronics. *Advanced Materials* **28**, 502-509 (2016).

73. B. Schazmann, D. Morris, C. Slater, S. Beirne, C. Fay, R. Reuveny, N. Moyna, D. Diamond, A wearable electrochemical sensor for the real-time measurement of sweat sodium concentration. *Analytical Methods* **2**, 342-348 (2010).

74. D. P. Rose, M. E. Ratterman, D. K. Griffin, L. Hou, N. Kelley-Loughnane, R. R. Naik, J. A. Hagen, I. Papautsky, J. C. Heikenfeld, Adhesive RFID sensor patch for monitoring of sweat electrolytes. *IEEE Transactions on Biomedical Engineering* **62**, 1457-1465 (2015).

75. J. Keller, C. Fibbe, F. Volke, J. Gerber, A. C. Mosse, M. Reimann-Zawadzki, E. Rabinovitz, P. Layer, D. Schmitt, V. Andresen, Inspection of the human stomach using remote-controlled capsule endoscopy: a feasibility study in healthy volunteers (with videos). *Gastrointestinal endoscopy* **73**, 22-28 (2011).

76. M. Camilleri, N. K. Thorne, Y. Ringel, W. L. Hasler, B. Kuo, T. Esfandyari, A. Gupta, S. M. Scott, R. W. McCallum, H. P. Parkman, Wireless pH-motility capsule for colonic transit: prospective comparison with radiopaque markers in chronic constipation. *Neurogastroenterology & Motility* **22**, 874-e233 (2010).

77. D. Cassilly, S. Kantor, L. Knight, A. Maurer, R. Fisher, J. Semler, H. Parkman, Gastric emptying of a non-digestible solid: assessment with simultaneous SmartPill pH and pressure capsule, antroduodenal manometry, gastric emptying scintigraphy. *Neurogastroenterology & Motility* **20**, 311-319 (2008).

78. M. Efentakis, J. Dressman, Gastric juice as a dissolution medium: surface tension and pH. *European journal of drug metabolism and pharmacokinetics* **23**, 97-102 (1998).

79. S. Maqbool, H. P. Parkman, F. K. Friedenberg, Wireless capsule motility: comparison of the SmartPill® GI monitoring system with scintigraphy for measuring whole gut transit. *Digestive diseases and sciences* **54**, 2167-2174 (2009).

80. A. Arshak, K. Arshak, D. Waldron, D. Morris, O. Korostynska, E. Jafer, G. Lyons, Review of the potential of a wireless MEMS and TFT microsystems for the measurement of pressure in the GI tract. *Medical engineering & physics* **27**, 347-356 (2005).

81. H. M. Fadda, M. C. Hernández, D. N. Margetson, S. M. McAllister, A. W. Basit, S. Brocchini, N. Suárez, The molecular interactions that influence the plasticizer dependent dissolution of acrylic polymer films. *Journal of pharmaceutical sciences* **97**, 3957-3971 (2008).

82. S. U. Schilling, H. L. Lirola, N. H. Shah, A. Waseem Malick, J. W. McGinity, Influence of plasticizer type and level on the properties of Eudragit® S100 matrix pellets prepared by hot-melt extrusion. *Journal of microencapsulation* **27**, 521-532 (2010).

83. J. P. Gong, Y. Katsuyama, T. Kurokawa, Y. Osada, Double-Network Hydrogels with Extremely High Mechanical Strength. *Advanced Materials* **15**, 1155-1158 (2003).

84. M. F. Butler, Y. F. Ng, P. D. Pudney, Mechanism and kinetics of the crosslinking reaction between biopolymers containing primary amine groups and genipin. *Journal of Polymer Science Part A: Polymer Chemistry* **41**, 3941-3953 (2003).